



**HAL**  
open science

## **Proteasomal degradation of retinoid X receptor alpha reprograms transcriptional activity of PPARgamma in obese mice and humans.**

Bruno Lefebvre, Yacir Benomar, Aurore Guédin, Audrey Langlois, Nathalie Hennuyer, Julie Dumont, Emmanuel Bouchaert, Catherine Dacquet, Luc Pénicaud, Louis Casteilla, et al.

### ► **To cite this version:**

Bruno Lefebvre, Yacir Benomar, Aurore Guédin, Audrey Langlois, Nathalie Hennuyer, et al.. Proteasomal degradation of retinoid X receptor alpha reprograms transcriptional activity of PPARgamma in obese mice and humans.. *Journal of Clinical Investigation*, 2010, 120 (5), pp.1454-68. 10.1172/JCI38606 . inserm-00472906

**HAL Id: inserm-00472906**

**<https://inserm.hal.science/inserm-00472906>**

Submitted on 13 Apr 2010

**HAL** is a multi-disciplinary open access archive for the deposit and dissemination of scientific research documents, whether they are published or not. The documents may come from teaching and research institutions in France or abroad, or from public or private research centers.

L'archive ouverte pluridisciplinaire **HAL**, est destinée au dépôt et à la diffusion de documents scientifiques de niveau recherche, publiés ou non, émanant des établissements d'enseignement et de recherche français ou étrangers, des laboratoires publics ou privés.

THE PROTEASOMAL DEGRADATION OF RETINOID X  
RECEPTOR $\alpha$  REPROGRAMS PEROXISOME PROLIFERATOR-  
ACTIVATED RECEPTOR  $\gamma$  TRANSCRIPTIONAL ACTIVITY IN  
OBESITY

**Bruno Lefebvre<sup>1,2,3,4,8,\*</sup>, Yacir Benomar<sup>1,2,3,4\*</sup>, Aurore Guédin<sup>1,2,3,4</sup>, Audrey  
Langlois<sup>1,2,3,4</sup>, Nathalie Hennuyer<sup>1,2,3,4</sup>, Julie Dumont<sup>1,2,3,4</sup>, Emmanuel  
Bouchaert<sup>1,2,3,4</sup>, Catherine Dacquet<sup>5</sup>, Luc Pénicaud<sup>6</sup>, Louis Casteilla<sup>6</sup>, Francois  
Pattou<sup>7</sup>, Alain Ktorza<sup>5</sup>, Bart Staels<sup>1,2,3,4</sup>, Philippe Lefebvre<sup>1,2,3,4,\$</sup>**

<sup>1</sup> Univ Lille Nord de France, F-59000, Lille, France ; <sup>2</sup> INSERM, UMR1011, F-59000, Lille, France ; <sup>3</sup> UDSL, F-59000, Lille, France ; <sup>4</sup> Institut Pasteur de Lille, F-59019, Lille, France; <sup>5</sup> Division of Metabolic Diseases, Institut de Recherches Servier, Suresnes, F-92150 France, <sup>6</sup> UMR 5241 CNRS-Université Paul Sabatier, IFR31, Toulouse, France. <sup>7</sup> INSERM U859, Faculté de Médecine de Lille-Pôle Recherche; 1 place de Verdun; F-59045 Lille cedex; France.

<sup>8</sup> Present address: INSERM U859, Faculté de Médecine de Lille-Pôle Recherche; 1 place de Verdun ; F-59045 Lille cedex; France.

\* BL and YB should be considered as equal contributors to this work.

Running title: ***UCH-L1 controls corepressor recruitment to PPAR $\gamma$ .***

<sup>\$</sup> Corresponding author: Philippe Lefebvre, Faculté de Médecine de Lille-Pôle Recherche; INSERM U545-Bâtiment J&K; Boulevard du Professeur Leclerc ; 59045 Lille cedex; France.  
Tel +33.3.20974220, Fax +33.3.20974201,  
e-mail: philippe-claude.lefebvre@inserm.fr

## SUMMARY

The chronic, low grade inflammation occurring in obese patients, which predisposes to type 2 diabetes, results in part from dysregulated visceral white adipose tissue functions. Here we report that the PPAR $\gamma$  signaling pathway operates differently in visceral WAT from lean mice vs. obese mice. An increased sensitivity of PPAR $\gamma$  to activation by its agonist the insulin sensitizer rosiglitazone was observed in visceral, but not subcutaneous obese WAT. This correlated to an increased expression of the gene encoding for ubiquitin hydrolase/ligase UCH-L1, and to an increased protein breakdown of the PPAR $\gamma$  heterodimerization partner RXR $\alpha$ , but not RXR $\beta$ , in visceral WAT from obese humans and mice. Interestingly, an increased UCH-L1 expression and concomitant proteasome-mediated breakdown of RXR $\alpha$ , but not of RXR $\beta$ , was induced in vitro by conditions mimicking hypoxia, as occurs in obese visceral WAT. Finally, only PPAR $\gamma$ -RXR $\beta$ , but not PPAR $\gamma$ -RXR $\alpha$  heterodimers efficiently dismissed the transcriptional corepressor SMRT upon agonist binding. As a consequence, an increased RXR $\beta$ :RXR $\alpha$  ratio resulted in increased PPAR $\gamma$  responsiveness upon agonist stimulation. Thus in obesity, the selective proteasomal degradation of RXR $\alpha$ , which is initiated by UCH-L1 upregulation, modulates the relative affinity of PPAR $\gamma$  heterodimers for SMRT, their responsiveness to PPAR $\gamma$  agonists and ultimately activates the PPAR $\gamma$ -controlled gene network in visceral WAT.

## INTRODUCTION

From a clinical perspective, visceral obesity predisposes to an increased incidence of type 2 diabetes mellitus (T2DM) and associated cardiovascular diseases (1;2). The visceral white adipose tissue depot (visWAT) is believed to contribute to the low grade, chronic inflammatory state which occurs in obese patients and animals and favors the progression towards T2DM. This feature stems from the specific functional properties of adipocytes from this WAT depot, which are highly sensitive to  $\beta$ -adrenergic stimulation and relatively resistant to the anti-lipolytic effects of insulin when compared to subcutaneous adipocytes (3). Indeed, while subcutaneous WAT (scWAT) is predominantly, but not exclusively, a lipid storage tissue exhibiting a high adipocyte plasticity, visWAT also triggers complex endocrine regulations by releasing free fatty acids (FFA), hormones and cytokines which reach the liver through the portal vein [reviewed in (4)]. How visWAT functions are affected upon disease progression is unknown, but metabolic challenges increase the release of proinflammatory cytokines and decrease that of insulin-sensitizing adipokines by visWAT.

Results from recent clinical trials [ADOPT, DREAM and PROACTIVE (5)] indicate that the insulin-sensitizers thiazolidinediones (TZDs) are highly efficient in maintaining glycemic control, and may exert pancreas-sparing and vascular protective effects in T2DM patients. TZDs are synthetic agonists for the Peroxisome Proliferator-Activated Receptor gamma (PPAR $\gamma$ /NR1C3), a member of the nuclear receptor superfamily. PPAR $\gamma$  is a key regulator of adipocyte differentiation and lipid storage, thereby exerting major effects on energy homeostasis (6). Gene ablation studies have confirmed the major role of adipocyte PPAR $\gamma$  (adPPAR $\gamma$ ) in mediating the insulin-sensitizing effect of TZDs in obese mice (7-12). Ligand-activated adPPAR $\gamma$  has a positive effect on glucose homeostasis by favoring scWAT expansion and FFA redistribution to this fat depot (13). Removing FFA from other tissues, including skeletal muscle and visWAT, prevents the so-called lipotoxic effect, which causes insulin resistance and hence translates into a greater insulin sensitivity. TZDs also act directly on visWAT functions by regulating the expression of adipokines (14) and several key metabolic genes (15). Quite intriguingly, however, TZDs do not exert detectable insulin sensitizing effects nor significant metabolic effects in lean individuals and mice, suggesting that the PPAR $\gamma$  pathway operates differently in normal and pathological conditions (16-18).

PPAR $\gamma$  activates target gene transcription by forming obligate heterodimers with the Retinoic X Receptor isotypes (RXR $\alpha$ , RXR $\beta$ , RXR $\gamma$ ) onto PPAR-responsive elements (PPRE). PPREs are found in genes controlling key steps in lipid and glucose metabolism, such as the

adipose-specific fatty acid binding protein (aP2), phosphoenolpyruvate carboxykinase (PEPCK) or lipoprotein lipase (LPL). Of note, RXR $\alpha$  also plays a critical role in adipogenesis *in vivo* (19). Agonist-mediated activation of PPAR $\gamma$  induces structural transitions occurring in the ligand-binding domain (LBD) of this receptor, creating a hydrophobic groove and a charge clamp which binds LXXLL motifs found in most coactivators (CoAs) such as the p160-related coactivator family (SRC1, 2 and 3) (20), the integrator complex CBP/p300 (21), components of the mediator complex (22) and the metabolically regulated coactivator PGC-1 $\alpha$  (23;24). Agonist-dependent CoA recruitment to PPAR $\gamma$  is concomitant to corepressor dismissal, and both the nuclear receptor corepressor (NCoR) and the silencing mediator for retinoic and thyroid receptor (SMRT) have been shown to impact on PPAR $\gamma$ -controlled cellular processes in distinct cellular backgrounds (25-27).

PPAR $\gamma$  transcriptional activity is therefore dependent on its sequential association with multiprotein complexes. It is thus likely that processes controlling protein stability and degradation also influence the overall activity of the PPAR $\gamma$  complex and may possibly impact on its function under conditions of obesity and T2DM. Indeed, components of the ubiquitin-proteasome system (UPS) have been shown to be involved in PPAR $\gamma$ -mediated transactivation (28). Although a few studies documented a dysregulated expression of several UPS components in cardiovascular diseases (29;30), a potential contribution of the UPS in the pathogenesis of T2DM and obesity remains unexplored. In this paper, we have investigated the relationship between metabolic states, UPS component expression and the PPAR $\gamma$  signaling pathway. We report that the expression of the ubiquitin hydrolase/ligase UCH-L1 is specifically and strongly upregulated in visWAT from obese patients and mice. Mimicking hypoxia *in vitro* also upregulated UCH-L1 expression. This enzyme promotes the selective breakdown of RXR $\alpha$ , which correlates with an increased response of PPAR $\gamma$  to a synthetic agonist *in vivo*. Moreover, decreasing the RXR $\alpha$ :RXR $\beta$  ratio *in vitro* resulted in an increased PPAR $\gamma$  transcriptional activity. The molecular basis of this phenomenon was found to be the result from a stable, ligand-insensitive tethering of SMRT to RXR $\alpha$ -PPAR $\gamma$  heterodimers.

## RESULTS

### **PPAR $\gamma$ target genes are more sensitive to agonist stimulation in visceral adipose tissue of obese, but not of lean mice.**

Since previous studies reported an unexpected insensitivity of lean mice or humans to TZD treatment, we investigated whether TZDs have a differential efficiency in normal (lean) vs. pathological (ob/ob) WAT. Treatment with rosiglitazone (RSG, 3mpk) lowered plasma glucose, insulinemia and to a lesser extent triglycerides in 10 week-old male ob/ob mice, but had no effect in lean OB/OB littermates (Supplementary Figure 1). This suggests that activation of PPAR $\gamma$  could induce distinct biological responses depending on the energetic status. To assess this at the molecular level, adipose tissue gene expression profiles were examined by oligonucleotide microarray analysis of visWAT mRNAs from OB/OB and ob/ob mice treated or not with RSG (Figure 1A). While these tissues exhibited similar PPAR $\gamma$  protein expression levels (Figure 1B), RSG upregulated (>1.5-fold,  $p < 0.05$ ) only 32 genes in OB/OB visWAT, whereas 153 genes were upregulated in ob/ob visWAT, a significant fraction of the latter being involved in metabolic control. Of these, only four genes were upregulated both in OB/OB and ob/ob visWAT, suggesting that PPAR $\gamma$  regulates distinct transcriptional networks in normal and pathological tissues. This was confirmed by a Gene Ontology functional classification. Importantly, upregulated genes in ob/ob visWAT included known direct target genes for PPAR $\gamma$  (CIDEA, UCP1, pyruvate carboxylase, malic enzyme...) which were not significantly upregulated in visWAT from lean animals. We thus compared the ability of RSG to induce a subset of PPRE-driven, adipocyte target genes in scWAT (inguinal) or visWAT (epididymal) from ob/ob mice and OB/OB littermates (Figure 1C) by real time PCR. While mRNA levels of the PPAR $\gamma$  target genes adiponectin, GyK, aP2, Glut4, PPAR $\gamma$  and PEPCK were upregulated to a similar extent in scWAT from OB/OB and ob/ob mice, they exhibited a much stronger responsiveness to RSG in visWAT from ob/ob mice (Figure 1C), in line with the microarray data. These comparative results thus demonstrate that PPAR $\gamma$  target genes are more sensitive to agonist-mediated activation in obese visWAT when compared to lean visWAT. In sharp contrast, such an activity shift was not observed in scWAT.

### **RXR $\alpha$ protein steady state levels are decreased in visceral adipose tissue of obese, but not lean humans and mice.**

PPAR $\gamma$  transcriptional activity depends on its association with a number of cofactors, including RXRs. We thus reasoned that the increased PPAR $\gamma$  transcriptional activity in obese visWAT might result from an altered expression of a PPAR $\gamma$  cofactor. A preliminary

characterization of the mRNA expression levels of several PPAR $\gamma$  primary cofactors did not reveal significant differences between lean and obese visWAT with the exception of PGC1 $\alpha$ , whose expression decreased by *ca.* 3 fold in obese visWAT (data not shown). We then monitored RXR $\alpha$ , RXR $\beta$  and RXR $\gamma$  mRNAs levels by qPCR in mouse inguinal (scWAT) and epididymal WAT (visWAT) depots (Figure 2A and 2B). RXR mRNA levels were similar in WAT of lean (OB/OB), obese (ob/ob), mice fed a regular diet (LFD) or high fat diet (HFD). However, RXR $\alpha$  activity has been shown to be regulated by protein degradation in several cell types (31-35). We thus investigated whether RXR $\alpha$  polypeptide stability could be affected in visWAT and scWAT of lean or obese mice. Immunohistochemical or western blotting analysis revealed that RXR $\alpha$  is expressed in adipocytes and preadipocytes of both visWAT and scWAT from OB/OB mice (Figure 2C). We thus quantified the expression level of RXR $\alpha$  and RXR $\beta$  polypeptides, which are the highest expressed in adipose tissues, in OB/OB and ob/ob mouse visWAT and scWAT (Figure 2D, left panels). Western blot analysis of mouse WAT extracts for RXR $\alpha$  and RXR $\beta$  revealed that RXR $\alpha$  expression is strongly diminished in ob/ob WAT epididymal tissue, whereas RXR $\beta$ , although less abundantly expressed, is expressed at similar levels in lean and obese WAT (Figure 2D left panels, Figures 2E and 2F). This altered expression was specific for visWAT, since scWAT from lean and ob/ob mice displayed similar RXR $\alpha$  and RXR $\beta$  levels. To rule out that RXR $\alpha$  downregulation is specific to the ob/ob genetic background, RXR $\alpha$  and RXR $\beta$  content were also quantified in WAT from mice fed either a low or high fat diet. Interestingly, RXR $\alpha$ , but not RXR $\beta$ , protein levels were also specifically decreased in visWAT from diet-induced obese mice (Figure 2D right panels, Figures 2E and 2F).

Similarly, we investigated whether RXR polypeptide stability could be affected in human scWAT and visWAT biopsies from patients with different levels of obesity and diabetes (Figures 2G, 2H). RXR $\alpha$ , RXR $\beta$  and RXR $\gamma$  mRNA levels did not differ between scWAT and visWAT biopsies from normal(L), obese (O), obese glucose-intolerant (OI), and obese diabetic (OD) individuals. Western blot analysis of WAT extracts for RXR $\alpha$  and RXR $\beta$  revealed that the RXR $\alpha$ , but not the RXR $\beta$  polypeptide, was much less abundant in visWAT from obese diabetic subjects than in visWAT from lean subjects (Figure 2I, 2J, 2K). In contrast, RXR $\alpha$  and RXR $\beta$  expression were not different in scWAT from lean vs. obese diabetic individuals (Figure 2I, 2J, 2K). Of note, PPAR $\gamma$  expression was comparable in all tissues (Figure 2I, 2L). Collectively, these findings show that the RXR $\alpha$  protein is specifically degraded in visWAT from obese humans and mice.

### **The expression of the ubiquitin esterase/ligase UCH-L1 is increased in visceral white adipose tissues of obese humans and mice.**

Since RXR $\alpha$  mRNA levels were not altered, we postulated that the severe decrease

in RXR $\alpha$  protein might stem from a dysregulated expression of component(s) of the ubiquitin-proteasome system (UPS) during metabolic disease progression. Therefore, the expression of UPS components was monitored in scWAT and visWAT from lean, obese, obese glucose-intolerant, and obese diabetic individuals. While the expression of components constituting the canonical 26S proteasome was not significantly altered in any of these WAT depots (data not shown), the expression of UCH-L1, an ubiquitin esterase/ligase enzyme, increased in visWAT but not in scWAT with progressing stages of the disease (Figure 3A and 3B). In contrast, the expression of other UPS components such as USP22 and WWP2, known to regulate the stability of transcription factors such as NF $\kappa$ -B or RNA polymerase 2, was not significantly modified. Since the dysregulated UCH-L1 expression was depot-specific in humans, we investigated whether a similar phenomenon occurs in mouse WAT tissues, by comparing the expression of UCH-L1, USP22 and WWP2 in WAT from wild type (OB), ob/ob (ob) or mice fed a high fat diet (HFD) (Figure 3C). Strikingly, a strong upregulation of UCH-L1 mRNA was observed in epididymal (visceral) WAT tissues of ob/ob and high fat-fed mice, whereas USP22 and WWP2 exhibited a less pronounced upregulation (5-fold vs. 2.5-fold). In contrast, the expression of these genes was similar in inguinal WAT of OB/OB, ob/ob and HFD mice. This upregulation was also observed at the protein level (Figure 3D). These data demonstrate that UCH-L1 is strongly and specifically upregulated in visWAT from metabolically challenged humans or mice.

### **RXR $\alpha$ polypeptide stability is altered by UCH-L1 upregulation and proteasomal degradation.**

The correlation between UCH-L1 upregulation and the strongly reduced RXR $\alpha$  polypeptide steady levels in obesity led us to speculate that UCH-L1 could be critical in controlling RXR $\alpha$  stability. We therefore transfected 3T3-L1 preadipocytes with expression vectors coding for RXR $\alpha$  or RXR $\beta$ , with or without an expression vector coding for UCH-L1 (Figure 4A). Incubation of RXR transfected cells with the proteasome inhibitor MG132 moderately increased the amount of RXR $\alpha$ , but did not influence RXR $\beta$  protein level. A combination of ammonium chloride and leupeptin (NH<sub>4</sub>/Leu), which inhibits the lysosomal degradation pathway, did not modify RXR $\alpha$  and RXR $\beta$  protein levels in RXR transfected cells. Quite remarkably, UCH-L1 overexpression in RXR transfected cells induced the breakdown of the RXR $\alpha$  polypeptide, whereas RXR $\beta$  stability was unaffected. UCH-L1-induced RXR $\alpha$  breakdown could be prevented by MG132 but not by NH<sub>4</sub>/Leu, indicating that UCH-L1 promotes RXR $\alpha$  breakdown through proteasomal degradation. RXR ubiquitylation was then examined in 3T3-L1 preadipocytes transfected with expression vectors coding for RXR and HA-tagged ubiquitin. Immunoprecipitation of RXR followed by

western blot detection of HA-tagged ubiquitin (Figure 4B) or immunoprecipitation of HA-tagged proteins followed by western blot detection of RXR (supplementary Figure 2) showed that only RXR $\alpha$  was intensively conjugated to HA-ubiquitin, and that UCH-L1 overexpression significantly increased ubiquitinylation of RXR $\alpha$ , but not of RXR $\beta$ . Furthermore, an in vitro ubiquitinylation assay using purified RXRs as substrates showed that RXR $\alpha$  was ubiquitinated in an ATP-dependent manner (Figure 4C). Ubiquitin-conjugated RXR $\alpha$  was stabilized in the presence of ubiquitin aldehyde, a general inhibitor of ubiquitin hydrolases (36), or of MG132. In sharp contrast, RXR $\beta$  was not detectably conjugated to ubiquitin in similar conditions (Figure 4B and supplementary Figure 2). Taken together, these data demonstrate that RXR $\beta$  is refractory to proteasome-mediated breakdown.

Hypoxia is a feature of obese WAT [reviewed in (37)], characterized by induced gene expression and protein stabilization of hypoxia-inducible transcription factors (HIF). Accordingly, HIF1 $\alpha$  mRNA was upregulated in visWAT from obese and HFD mice (Figure 4D), whereas the expression of HIF1 $\beta$  and HIF2 $\beta$  was selectively increased in visWAT from HFD mice. HIF2 $\alpha$  expression was unaffected in both types of WAT. Since HIF1 $\alpha$  upregulation in obese WAT correlated with increased UCH-L1 expression (Figure 3C), and given the occurrence of several HIF-response elements in the promoter of the mouse and human UCH-L1 genes, we tested whether cobalt chloride (CoCl<sub>2</sub>), an hypoxia-mimicking compound, also upregulated UCH-L1 in differentiated 3T3-L1 adipocytes. CoCl<sub>2</sub> caused a concomitant upregulation of HIF1 $\alpha$  and UCH-L1 mRNAs (Figure 4E), and a dose-dependent degradation of the RXR $\alpha$  protein (Figure 4F). Furthermore, MG132 and LDN-54777, a specific inhibitor of UCH-L1 (38), blocked the CoCl<sub>2</sub>-induced RXR $\alpha$  degradation in a dose-dependent manner (Figure 4G).

Pulse-chase labeling of 3T3-L1 adipocyte proteins showed that the decay of RXR $\alpha$  was linear, with a half life of about 8 hours (Figure 4H). CoCl<sub>2</sub> treatment decreased the half life of RXR $\alpha$  to 4 hours, whereas LDN-54777 clearly prevented the CoCl<sub>2</sub>-induced RXR $\alpha$  breakdown ( $t_{1/2}$ =7 hours). Taken together, these data argue for a role of UCH-L1 in the UPS-mediated RXR $\alpha$  degradation process, in which hypoxia might play a role.

### **The RXR $\alpha$ :RXR $\beta$ ratio determines PPAR $\gamma$ responsiveness to agonist in murine adipocytes.**

In light of the above results, we investigated whether an altered RXR $\alpha$  to RXR $\beta$  ratio might directly alter PPAR $\gamma$  responsiveness to agonist challenge in a cell-autonomous manner. RXR $\alpha$  is strongly expressed in 3T3-L1 differentiated adipocytes, whereas RXR $\beta$  and RXR $\gamma$  are expressed at much lower levels (Figure 5A). PPAR $\gamma$ , as well as PPAR $\alpha$ , are

also expressed in differentiated 3T3-L1 cells. RSG treatment readily activated aP2, GyK and adiponectin gene expression (Supplementary Figure 3). ChIP assays using anti-RXR or anti-PPAR antibodies (Figure 5B) failed to detect RXR $\gamma$  on the aP2 and adiponectin PPREs, in agreement with its low expression level, whereas a comparable occupancy by both RXR $\alpha$  and RXR $\beta$  could be detected on these promoters. PPAR $\gamma$ , but not PPAR $\alpha$ , bound also to these promoters, and PPAR $\gamma$  and RXRs density on these promoters were similar in the absence and presence of RSG (Figure 5B). Identical results were obtained for the Gyk promoter (data not shown). Thus simultaneous expression of RXR $\alpha$  and RXR $\beta$  generates PPAR $\gamma$ -driven promoters on which both RXR isotypes can be loaded.

To further assess the role of the RXR isotype on aP2, adiponectin and GyK gene responsiveness to RSG, we generated RXR $\alpha$ -depleted 3T3-L1 adipocytes by siRNA-mediated knockdown, which induced a specific RXR $\alpha$  mRNA decrease of 70% (Supplementary Figure 4). RXR $\alpha$  knockdown resulted in a more pronounced induction of the PPAR $\gamma$ -target genes by rosiglitazone (aP2: 9.0 vs 3.6-fold induction; adiponectin: 4.6 vs 2.6-fold induction and GyK: 6.3 vs 4.4-fold induction, Figure 5C). Conversely, 3T3-L1 CAR cells, which stably overexpress the adenovirus receptor (39), were differentiated into adipocytes and transduced at day 6 with adenoviral particles encoding either GFP as a negative control, RXR $\alpha$  or RXR $\beta$ , allowing a strong overexpression of each RXR isotype (Supplementary Figure 5). Interestingly, RSG treatment resulted in a stronger induction of aP2, adiponectin, GyK and PPAR $\gamma$  in RXR $\beta$ -overexpressing cells compared to GFP-expressing cells (Figure 5D). Inversely, forced expression of RXR $\alpha$  attenuated the induction of PPAR $\gamma$  target genes by RSG (Figure 5D).

### **The RXR $\alpha$ :RXR $\beta$ ratio determines PPAR $\gamma$ responsiveness to agonist in different cellular backgrounds.**

We further investigated whether a decreased RXR $\alpha$  expression would cause a derepression of PPAR $\gamma$  target genes in other cellular backgrounds exhibiting varying ratios of RXR $\alpha$  to RXR $\beta$ , as assessed by Q-PCR analysis (Figure 5E). 3T3-L1 preadipocytes displayed a RXR $\alpha$ :RXR $\beta$  mRNA ratio of 10 to 1, much like the HepG2 hepatocarcinoma (10:1) and the C2C12 myeloblastic (4:1) cell lines. In contrast, the  $\beta$ -insulinoma cell line Min6 expressed comparable levels of RXR $\alpha$  and RXR $\beta$  mRNAs (1:1). Assessment of the transcriptional activity of PPAR $\gamma$  in these different cell types using the J6 tk-Luc reporter gene showed that a much higher maximal transcriptional activity was reached in Min6 cells than in 3T3-L1, C2C12 and HepG2 cells in response to rosiglitazone (Figure 5F). Overexpressing RXR $\alpha$  in Min6 cells significantly blunted the response to rosiglitazone, whereas overexpression of RXR $\beta$  potentiated this response (Figure 5G). A similar pattern

was obtained in COS cells and on another PPRE-driven reporter gene (ApoA2-tk Luc), showing that the RXR $\alpha$  repressive function is neither dependent on the cell type nor on the response element (Figure 5H). We then used a system in which the P box, located in the DNA binding domain of either RXR $\alpha$  or RXR $\beta$ , was mutated to confer a high affinity for a glucocorticoid responsive element (GRE) half-site. The RXR binding polarity can thus be imposed when using a chimeric DR1 PPRE in which the GRE half site is either located in 3' or 5'. This system is only functional when RXR is bound on the 3' half-site of the chimeric PPRE [(40) and Figure 5I]. In this configuration, PPAR $\gamma$  was more sensitive to a moderate RSG concentration (30nM) when RXR $\beta$  was expressed (Figure 5I).

Taken together, these data indicate that (i) PPAR $\gamma$  can bind as a dimer with RXR $\alpha$  or RXR $\beta$  to PPRE-driven promoters in adipocytes; (ii) this interaction is not ligand-sensitive, and (iii) a decreased RXR $\alpha$  expression correlates in vitro and in vivo to an increased responsiveness to rosiglitazone. RXR $\alpha$  thus acts as a repressor of PPAR $\gamma$  responsiveness to agonist challenge in murine adipocytes.

### **Corepressors interact with PPAR $\gamma$ in vitro and in intact cells.**

Taken collectively, these results show that RXR $\alpha$ /PPAR $\gamma$  heterodimers display a lower sensitivity to agonist challenge than RXR $\beta$ /PPAR $\gamma$  dimers. To test whether this might be due to an increased interaction with nuclear receptor corepressors, the influence of the RXR isotype on the binding of PPAR $\gamma$  to SMRT or NCoR was further characterized. A yeast two-hybrid assay was first performed to assess the interaction of PPAR $\gamma$  fused to the Gal4 DNA binding domain (DBD), with the nuclear receptor interaction domain (NRID) of either SMRT (AAs 2061 to 2472) or NCoR (AAs 1906 to 2313) fused to the NF-kappa-B activation domain. SMRT interacted more efficiently with the PPAR $\gamma$  LBD than NCoR, whereas the interaction of the PPAR $\gamma$  LBD with the coactivator Med1/TRAP220/DRIP205 was negligible (Figure 6A). Performing a similar two-hybrid assay in mammalian HeLa cells using the PPAR $\gamma$  ligand binding domain (LBD) fused to the Gal4 DBD and NRIDs fused to the VP16 activation domain (AD) revealed a similar pattern of interaction (Figure 6B), demonstrating that the preferential interaction of SMRT with PPAR $\gamma$  is an intrinsic property not affected by the cellular background. SMRT was therefore selected as the representative corepressor in further experiments.

A GST-pulldown assay was then carried out to assess the interaction between full length PPAR $\gamma$  and SMRT. Using an immobilized glutathione S-transferase (GST)-SMRT fusion protein and radiolabeled PPAR $\gamma$ , a strong interaction was detected between the two proteins in this system (Figure 6C). Rosiglitazone (Figure 6C) and two other PPAR $\gamma$  agonists, pioglitazone and troglitazone (Supplementary figure 6A), were unable to promote

a significant release of SMRT from monomeric PPAR $\gamma$ . In similar conditions, rosiglitazone promoted the recruitment of Med1/DRIP205/TRAP220, GRIP1/TIF-2 and PGC-1 $\alpha$  to the PPAR $\gamma$  LBD (Supplementary figure 6B), showing that the PPAR $\gamma$  LBD undergoes appropriate structural transitions. Thus the PPAR $\gamma$ -SMRT interaction is not sensitive to PPAR $\gamma$  agonist binding in this setting. To assess whether a stable interaction with SMRT also occurred on PPAR $\gamma$  target gene promoters, ChIP assays were performed in 3T3-L1 adipocytes. 3T3-L1 cells express several coactivators, as well as NCoR and SMRT whose mRNA expression levels do not vary significantly during the differentiation process (Supplementary figure 7). In differentiated, non stimulated 3T3-L1 adipocytes, SMRT was clearly detected on each promoter, whereas NCoR displayed a barely detectable binding (Figure 6D). Upon rosiglitazone treatment, SMRT was partially dismissed from both promoters, indicating that, in the context of an endogenous functional promoter, agonist-activated PPAR $\gamma$  is able to release, at least partially, SMRT. To confirm these findings, we monitored the association of two SMRT-associated proteins, HDAC3 and SIRT1. Similar to SMRT, both HDAC3 and SIRT1 were partially dismissed from the aP2 and adiponectin promoters (Figure 6E). Thus a partial, agonist-induced dismissal of corepressor complex correlates with a mixed RXR $\alpha$ /RXR $\beta$  occupancy at PPAR $\gamma$ -regulated target genes (Figure 5B).

#### **The RXR isotype affects SMRT interaction with the PPAR $\gamma$ -RXR heterodimer.**

We thus hypothesized that the increased RXR $\beta$ /PPAR $\gamma$  responsiveness to agonist could result from a specific feature of the RXR $\alpha$ :SMRT interaction. This hypothesis was tested using a two-hybrid assay in NIH-3T3 cells, which expresses neither PPAR $\gamma$  nor C/EBP $\alpha$  but can be fully differentiated into adipocytes upon ectopic expression of these two transcription factors (41) (Figure 7A). A Gal4-SMRT NRID fusion protein was overexpressed together with a PPAR $\gamma$  LBD-VP16 activating domain (AD) fusion protein, in the presence or not of either RXR $\alpha$  or RXR $\beta$ . The transcriptional activity of the system was monitored with a UAS-tk Luc reporter gene, whose activity is predicted to decline upon dissociation of the PPAR $\gamma$ -VP16 protein. As a control experiment, we expressed a hRAR $\alpha$ -VP16 fusion protein together with the Gal4-SMRT NRID. This system displayed a clear agonist (*all trans* retinoic acid, atRA)-dependent decreased transcriptional activity, hence reflecting the dissociation of the hRAR $\alpha$ -VP16 fusion protein from the Gal4-SMRT bait upon agonist binding (Figure 7A). In similar conditions, the PPAR $\gamma$ -VP16/Gal4-SMRT interaction was not sensitive to increasing concentrations of rosiglitazone. Concomitant overexpression of either RXR $\alpha$ , RXR $\beta$  or RXR $\gamma$  increased the basal level of interaction of PPAR $\gamma$  with SMRT. However, rosiglitazone induced a decreased activity of the system only in the presence of RXR $\beta$ , evidencing a decreased SMRT association with the PPAR $\gamma$ /RXR $\beta$

heterodimer. Taken together, these data suggest that the PPAR $\gamma$ -SMRT interaction is disrupted by rosiglitazone only when RXR $\beta$  is integrated in the ternary SMRT/PPAR $\gamma$ /RXR complex.

### **The RXR isotype impacts on SMRT-mediated repression of PPAR $\gamma$ .**

We concluded from ChIP and 2-hybrid data that the RXR $\alpha$ -PPAR $\gamma$  interaction with SMRT is ligand-insensitive. To validate further this hypothesis in the context of a DNA-bound PPAR $\gamma$ -RXR heterodimer, we used a modified two-hybrid assay in NIH 3T3 cells. The J6 tk-Luc reporter gene was cotransfected with PPAR $\gamma$  and RXR expression vectors, together with an expression plasmid coding either for VP16-AD as a control, or for a SMRT/VP16-AD fusion protein (noted VP16-SMRT in Figure 7B). Preliminary experiments showed that detected responses necessitated a PPRE sequence (data not shown). We first used the RAR $\alpha$ -RXR $\alpha$  heterodimer as a control system. The basal level of activity of this dimer was strongly increased in the presence of VP16-SMRT, indicative of a RAR $\alpha$ -RXR $\alpha$ /SMRT interaction. A saturating concentration of *atRA* (1 $\mu$ M) yielded a luciferase activity similar to that observed in control conditions (AD only), showing that SMRT is fully dissociated from the RXR-RAR complex upon agonist binding (Figure 7B). When transposed to the PPAR $\gamma$ -RXR $\alpha$  system, VP16-SMRT expression also strongly increased the basal activity of the reporter gene (5-fold induction) when compared to VP16-AD ("AD only"). However, in contrast to the RXR $\alpha$ -RAR $\alpha$  dimer, a higher transcriptional activity of the PPAR $\gamma$ /RXR $\alpha$  dimer when compared to control conditions (AD only) was maintained even at saturating RSG concentration. This additive induction is due to the cumulative effect of the AF2- and of the VP16-mediated transcriptional activation domains, strongly suggesting that agonist treatment does not induce the dismissal of VP16-SMRT from the PPAR $\gamma$ -RXR $\alpha$  heterodimer. RXR $\gamma$  exhibited a behavior similar to that of RXR $\alpha$  (Figure 7C). In sharp contrast, RXR $\beta$  overexpression generated a system in which saturating rosiglitazone concentrations prevented SMRT-VP16 to further activate the activity of the reporter gene, showing that the liganded RXR $\beta$ -PPAR $\gamma$  dimer cannot bind the SMRT moiety. We conclude from the above data that only the RXR $\beta$ -PPAR $\gamma$  dimer fully releases SMRT upon agonist binding.

## DISCUSSION

The transcriptional control of programs regulating metabolic homeostasis can be significantly altered by manipulating the activity of transcription factors belonging to the nuclear receptor (NR) superfamily. Amongst the NRs, PPAR $\gamma$  plays a very important role as it is a central regulator of lipid and glucose metabolism, and is important for maintaining whole body insulin sensitivity (42). However, how its function may be modulated upon disease progression is unknown. Our study provides a novel paradigm on how a transcriptional regulator may adjust its transcriptional activity in face of metabolic challenges.

The inverse correlation in visceral WAT from obese mice and humans between UCH-L1 expression and RXR $\alpha$  polypeptide stability highlights a novel regulatory mechanism of the PPAR $\gamma$  signaling pathway. UCH-L1 exhibits ubiquitin C-terminal hydrolase activity which, by maintaining a sufficient pool of cellular ubiquitin, sustains protein degradation. Additional roles such as ubiquitin ligation and stabilization of mono-ubiquitin have been described for UCH-L1 (reviewed in (43)). UCH-L1 substrates are unknown, but its involvement in the regulation of NF- $\kappa$ B activity in vascular cells (44) and variation of UCH-L1 gene expression in rat pancreatic islets exposed to high glucose concentrations (45) hint at a role in metabolic control. Although we found that UCH-L1 expression is increased at various stages of disease progression in humans, the mechanism leading hereto is unknown. Affecting obese WAT (37), hypoxia may be a possible link between pathological states and increased UCH-L1 expression. In addition, hypoxia has been reported to promote RXR $\alpha$  breakdown in cardiac myocytes (46). *ob/ob* and HFD epididymal WAT exhibit an increased expression level of HIF1 $\alpha$ , and the UCH-L1 promoter contains several HIF-response elements. In good agreement, we observed that cobalt chloride, an agent mimicking partially hypoxia through HIF1 $\alpha$  induction and stabilization, was able to increase UCH-L1 expression in 3T3-L1 adipocytes and to promote RXR $\alpha$  protein breakdown in a UCH-L1-dependent manner. RXR $\alpha$  is a known target of the UPS in several cell types (31-35), and our data show that RXR $\alpha$  is a substrate for *in vitro* ubiquitin conjugation, whereas RXR $\beta$  is unable to undergo this post-translational modification. However, recombinant UCH-L1 neither modified the ubiquitin conjugation rate in the acellular system, nor engaged direct protein-protein interaction with RXR $\alpha$  *in vitro* as assayed by GST pulldown assays (data not shown), suggesting that this enzyme promotes RXR $\alpha$  breakdown in an indirect manner. Combined with the fact that visWAT from *ob/ob* mice is more sensitive to TZD treatment than visWAT from *OB/OB* mice, our data raised the possibility that an UCH-L1-dependent RXR expression isotype switch could control PPAR $\gamma$  transcriptional

activity.

As all other ligand-regulated NRs, PPAR $\gamma$  exerts its transcriptional activity through the recruitment of coactivators, and PPAR $\gamma$  has been documented to bind in vitro to a variety of primary coactivators. PPAR $\gamma$  transcriptional activity is also modulated by corepressor recruitment, and we show herein that PPAR $\gamma$ -containing heterodimers recruit preferentially SMRT vs. NCoR. Such a preference has been already reported in a variety of cell-free and cellular systems by some (25;40;47;48) but not confirmed by others (26;49). Although RNA interference studies showed that SMRT represses PPAR $\gamma$  transcriptional activity (data not shown), we found that the physical interaction of PPAR $\gamma$  with SMRT is not affected by agonist binding. Thus assays involving solely PPAR $\gamma$  lack a critical component required for the ligand-regulated association of SMRT to PPAR $\gamma$ , in line with a previous report (50). As an obligate heterodimerization partner conferring specific DNA binding activity to PPAR $\gamma$ , RXR is a major regulator of PPAR $\gamma$  activity. Mammalian 2-hybrid assays established that RXR association to PPAR $\gamma$  allowed for a reversible association of SMRT to the PPAR $\gamma$ /RXR heterodimer in an isotype-dependent manner. Only RXR $\beta$  generated a complex able to dismiss SMRT in an agonist-dependent manner, providing a molecular basis for the higher inducibility of PPAR $\gamma$  in RXR $\beta$ -enriched cellular backgrounds. This was also true in a mouse adipocyte background, in which RXR $\alpha$  and RXR $\beta$  normally associate to the PPRE of PPAR $\gamma$  target genes. The interaction of PPAR $\gamma$ , as well as that of RXRs, with the PPRE of the endogenous  $\alpha$ 2, adiponectin and GyK gene promoters is constitutive and ligand-insensitive in differentiated 3T3-L1 adipocytes, in agreement with previous data (26). The mixed composition of PPRE-bound heterodimers led to the prediction, when considering our interaction data, that SMRT would be only partially released upon agonist challenge. This was indeed the case, and confirmed by the partial release of two SMRT-interacting proteins, HDAC3 and Sirt1. In agreement with the repressive role of RXR $\alpha$ , siRNA-mediated decrease of RXR $\alpha$  expression led to a higher sensitivity to rosiglitazone, and conversely, its overexpression in 3T3-L1 adipocytes and other cellular backgrounds invariably blunted responsiveness to rosiglitazone. A differential affinity of nuclear receptors for distinct corepressors has only been documented for NRs expressed as monomers. For example, a restricted SMRT recruitment has been observed for the *all trans* retinoic acid receptors RAR $\alpha$ , RAR $\beta$  and RAR $\gamma$  (51;52) and differences are due to the poorly conserved C-terminal F domain (53). However, since neither RXRs nor PPAR $\gamma$  have a F domain, other structural determinants must regulate the differential affinity of RXR $\alpha$ - vs. RXR $\beta$ -containing heterodimers for SMRT and are yet to be identified.

It has been postulated that the tissue-specific recruitment of nuclear coactivators by specific agonists influences PPAR $\gamma$  transcriptional activity, a mechanism *via* which

side-effects triggered in TZD-target tissues such as kidney, bone or even adipose tissues could be circumvented [see for examples (54-56)]. Our data suggest that PPAR $\gamma$  operates differently in normal and in pathological tissues due to heterodimerization with distinct RXR isotypes. Whether this phenomenon impinges also on the ability of PPAR $\gamma$  to recruit a specific subset of coactivators is unknown, but nevertheless underlines the need for a careful selection of screening procedures aiming at identifying novel PPAR $\gamma$  synthetic ligands. It also leaves open the possibility to design ligands favoring, or not, the heterodimerization with RXR $\alpha$ , thereby predictably moderating the transcriptional response to synthetic PPAR $\gamma$  ligands. The need for a moderated PPAR $\gamma$  activation has already been underlined by (i) the protective effect of the transcriptionally-altered Pro12Ala PPAR $\gamma$  mutant against the development of insulin resistance and type 2 diabetes, (ii) the improved insulin sensitivity of heterozygous PPAR $\gamma$ <sup>+/-</sup> mice fed a high fat diet and (iii) the beneficial effects on obesity and insulin resistance upon treatment with PPAR $\gamma$  antagonists (57)

In summary, our studies elucidated an unexpected mechanism by which the UPS regulates PPAR $\gamma$  transcriptional activity in pathological states, through a selective degradation of RXR $\alpha$ . Modifying PPAR $\gamma$  transcriptional activity in face of metabolic challenges may be a mechanism by which cells adapt to novel conditions through transcriptional reprogramming. Whether RXR $\alpha$ - and RXR $\beta$ -containing heterodimers control an overlapping or a specific transcriptional program is under investigation. A better understanding of the yet putative specific roles of RXR isotypes and of their regulation in pathological conditions may help defining new therapeutical strategies to treat type 2 diabetes and associated comorbidities.

## MATERIAL and METHODS

**Chemicals:** Isobutylmethylxanthine (IBMX), insulin, dexamethasone and atRA were obtained from Sigma (St. Quentin-Fallavier, France). LDN-57444 was purchased from Calbiochem. Rosiglitazone was synthesized at Servier's chemical facilities.

**Plasmids:** pSG5-hRAR $\alpha$ , pSG5-hRXR $\alpha$ , pSG5-hRXR $\beta$ , pSG5-hRXR $\gamma$ , pSG5-hPPAR $\gamma$ , (DR5)3-tk luc, VP16-hRAR $\alpha$ , (PPRE)6-tk luc and Gal4-tk luc were described elsewhere (58-61). VP16-PPAR $\gamma$  was kindly provided by B. M. Forman (62). Gal4-hSMRT(2117-2357) and VP16-hSMRT(2117-2357) were kind gifts from A.N. Hollenberg (25). pCMX-VP16-NCoR (1585-2453) was kindly provided by R. Renkawitz and M. Schulz (63). The pCMV-based human UCH-L1, USP22 and WWP2 expression vectors were purchased from OriGene (Rockville, MD USA).

**Cell culture and transfection:** NIH3T3 cells were grown in Dulbecco's modified Eagle medium (Glutamax-1, high glucose, Invitrogen) supplemented with 10% fetal calf serum (Biowhittaker) and 100U/mL penicillin and 100 $\mu$ g/mL streptomycin (Invitrogen). Transient transfection experiments were performed using Lipofectamine 2000 (Invitrogen). Luciferase assays were performed with the dual luciferase assay system (Promega) according to the manufacturer's guidelines.

Adipocyte differentiation was induced as follows: 3T3-L1 preadipocytes were cultured in DMEM supplemented with 10% fetal calf serum until they reached confluence. The medium was then changed and cells were allowed to grow for two additional days. Adipocyte differentiation was then induced by replacing the culture medium by DMEM supplemented with 10% FCS, 0.5mM isobutyl-methyl-xanthine (IBMX), 1 $\mu$ M dexamethasone and 10 $\mu$ g/mL insulin. Two days later, the medium was replaced with DMEM supplemented with 10% FCS and 10 $\mu$ g/mL insulin for two additional days. Cells were then re-fed at 48 hours intervals with DMEM supplemented with 10% FCS only.

**Pulse-chase labeling and immunoprecipitation:** Differentiated 3T3-L1 cells were starved in methionine/cysteine-free DMEM supplemented with glutamine and 10% dialyzed fetal calf serum for 4 hours. [<sup>35</sup>S] methionine and cysteine (250 $\mu$ Ci, EasyTag™ EXPRESS<sup>35</sup>S Protein Labeling Mix, Perkin-Elmer) was added to the culture medium for 4 hours. Two hours prior to the end of the pulse, 500 $\mu$ M CoCl<sub>2</sub> or/and 10 $\mu$ M LDN57444 was added to the medium. Radioactive media was removed and substituted for regular medium supplemented with 2mM cysteine and methionine, CoCl<sub>2</sub> or/and LDN57444. At the

indicated times, ca.  $10^7$  cells were collected in ice-cold 1x PBS, centrifuged and lysed into 500 $\mu$ L RIPA buffer (50mM Tris-HCl, pH 7.4, 150mM NaCl, 1% NP-40, 0.5% deoxycholate, 0.1% SDS, 10 $\mu$ g/mL leupeptin, 10 $\mu$ g/mL pepstatin, 5 $\mu$ g/mL aprotinin, 5mM DTT, 5mM PMSF, 1mM benzamide). The homogenate was spun down and the supernatant precleared with a protein A/protein G sepharose mix. The supernatant was incubated overnight at 4°C with 5 $\mu$ g of anti-RXR $\alpha$  antibody ( $\Delta$ N-197, sc-774, Santa Cruz Biotech.). Complexes were precipitated with a protein A/protein G mix, washed and analyzed by 8%SDS-PAGE.

**In vitro ubiquitin conjugation:** In vitro ubiquitinylation assays were carried out using a S100 HeLa cell extract and reagents according to the manufacturer's instructions (Enzo Life Sciences).

**In vivo ubiquitin conjugation:** 3T3-L1 preadipocytes were transfected with expression vectors encoding HA-tagged ubiquitin [MT123-Ub HA (64;65)], RXR $\alpha$  or RXR $\beta$ . Twenty four hours after transfection, whole cell extracts were prepared in RIPA buffer supplemented with 10 $\mu$ M MG132 and HA-tagged proteins were immunoprecipitated using an anti-HA tag antibody (ab9110, Abcam) or anti-RXR antibodies (see references below). Ubiquitinated RXR was detected by Western blotting using either anti-RXR or anti-HA tag antibodies as indicated in the figure legends.

**Immunofluorescence and western blot:** The anti-RXR $\alpha$  antibody used in immunochemistry experiments was from Perseus (PP-K8508-00). Adipose tissue was embedded in paraffin and sectioned (7 $\mu$ m). Sections were deparaffinised and rehydrated. After brief heating, the endogenous peroxidase activity was quenched and sections were then incubated with the anti-RXR antibody (1:200). Sections were then incubated with biotinylated goat anti-mouse antibody then with streptavidin-horseradish peroxidase (Vectastain). Antigenic complexes were detected with 3,3'-diaminobenzidine and sections were mounted in Mowiol. Images were collected with a Leica microscope and a camera coupled to the Leica IM500 image Manager software with a x10 magnification.

Primary antibodies used in western blotting experiments were directed against RXR $\alpha$  (Santa Cruz Biotech., D-20, sc-553), RXR $\beta$  (Santa Cruz Biotech., C-20, sc-831), RXR $\gamma$  (Santa Cruz Biotech., Y-20, sc-555), PPAR $\gamma$  (Santa Cruz Biotech., H-100, sc-7196) and UCH-L1 (Cell Signaling Tech., 3525S). Secondary antibodies coupled to HRP were from Sigma. Immune complexes were detected using the ECL+ system from Amersham/GE Healthcare

**Yeast interaction assays:** Yeast 2-hybrid experiments were carried out as described in Carmona et al. (54) at Phenex GmbH, Germany.

**ChIP assays:** ChIP assays were carried out as described previously (58;66). Primer sequences used in ChIP assays were described elsewhere (26) except for the adiponectin promoter region (forward primer 5'- CCATGCCTGCAGTCCATCTA-3' and reverse primer 5'- GCTTCTGTCAAGCCATCCTGT-3'). The antibody to SMRT (PA1-844A) was from Affinity Bioreagents, whereas anti-NCoR (sc-1609), -PPAR $\alpha$  (sc-9000), -PPAR $\gamma$  (sc-7196), -RXR $\alpha$  (sc-553), -RXR $\beta$  (sc-831) and -RXR $\gamma$  (sc-555) were purchased from Santa Cruz Biotechnology, Inc.

**GST-pulldown assays:** GST-pulldown experiments were performed as described previously (67). Data were acquired on a Storm 860 phosphorimager and band intensities were quantified using the ImageQuant TL software

**RNA extraction, Affymetrix analysis and real-time PCR:** Total RNA was prepared using the RNeasy minikit (Qiagen). Total RNA was isolated from mouse adipose tissues or from 3T3-L1 cells using the RNAeasy Lipid Tissue kit (Qiagen). Purified RNA was adjusted to 1 $\mu$ g/ $\mu$ L and its integrity was assessed by gel electrophoresis or on an Agilent Bioanalyzer. RNA was purified from visWAT from 3 mice from each group (OB/OB, OB/OB+RSG, ob/ob; ob/ob+RSG) and hybridized to Affymetrix 430 2.0 arrays after cDNA labeling. Data were analyzed using the GeneSpring GX software (Agilent). Normalization was performed using the RMA algorithm, followed by a Benjamini-Hochberg FDR statistical analysis. Genes that were significantly upregulated or repressed by more than 1.5-fold were then classified by a Gene Ontology functional classification. For RT-qPCR analysis of transcripts, reverse transcription was performed using random hexamers as recommended by the manufacturer (Promega). cDNAs were analyzed by PCR amplification using the TaqMan PCR master mix (Applied Biosystems) and a mix of actin primers and appropriate FAM probes. Absolute quantification of RXR mRNAs were determined by generating standard curves with known amounts of cloned RXR cDNAs. Actin, aP2, GyK, adiponectin primers and all other probes were purchased from Applied Biosystems (Assay on Demand). PCR (40 cycles) and data analysis were carried out using an ABI Prism 7500 (Perkin-Elmer).

**RNA interference:** Specific siRNA duplexes targeting RXR $\alpha$ , SMRT and non-specific siRNA controls were synthesized by Santa Cruz Biotech. siRNA were transfected using the

DeliverX Plus siRNA transfection kit (Panomics) according to the manufacturer's guidelines.

**Animal experiments:** OB/OB and ob/ob mice (8-10 weeks old) were purchased from Charles River (France). Mice were housed in a temperature-controlled room (22-24°C), with a relative humidity of 36-80% and 12 hours light/dark cycles (light 7:00 am to 7:00 pm). Mice were fed ad libitum with free access to filtered tap-water (0.22µm filter) and received irradiated pelleted laboratory chow (Ref# A03-10, UAR, France) throughout the study, supplemented or not with rosiglitazone to achieve a 3mpk/day intake. Mice were euthanized by cervical dislocation, and visceral and inguinal adipose tissues were dissected, weighed and immediately stored in liquid N<sub>2</sub>. All procedures were validated by the ethical committee of the Institut Pasteur de Lille and carried out in accordance with European Union (EEC/No. 07430) and French ethical guidelines.

**Isolation of stromal vascular fraction from adipose tissues:** Cells were prepared from adipose tissues of obese or control mice according to (68) with minor modifications. Briefly, tissue was digested at 37°C in 1x PBS containing 0.2% BSA and 2mg/mL collagenase (type II collagenase, Sigma). After filtration of the homogenate through 25µm filters, mature adipocytes were separated from pellets [stroma-vascular fraction, (SVF)] by centrifugation (600 g, 10 min.). After red cell lysis in 140mM NH<sub>4</sub>Cl and centrifugation, SVF cells were pelleted and resuspended in 1x PBS. Cells were seeded at 10,000 cells/cm<sup>2</sup> in DMEM-F12 supplemented with 10% newborn calf serum. Extensive washes were performed 12 hours later and whole cell lysates prepared 48 hours later.

**Human tissues:** Human white adipose tissue samples were collected from patients undergoing abdominal surgery by laparoscopy or coelioscopy after informed consent. All procedures were compliant to the French National Ethics Committee guidelines. Tissue samples from female patients with an age ranging from 35 to 59 years, and not receiving any oral antidiabetic treatment, were removed within the first 30 minutes of the surgical procedure and immediately frozen in liquid nitrogen. Visceral fat was removed from the great omentum and the subcutaneous fat was taken in the vicinity of the laparotomy incision. Based on biochemical and morphological parameters, patients were classified as lean (normal) (BMI<25; fasting glucose 6mM and OGTT <7.8mM); obese (BMI>35; FG<6mM, OGTT<7.8mM); obese and glucose intolerant (BMI>35, 6mM<FG<7mM, 7.8mM<OGTT<11.1mM) and obese diabetic (BMI>35, FG>7mM, OGTT>11.1mM). Glycemia was assayed, in the OGTT test, 120 minutes after the glucose load.

**Statistical analysis:** Data are means +/- SEM. Calculations were carried out using Prism software (GraphPAD Inc., San Diego, CA). Q-PCR, western-blot and transient transfection experiments were analyzed with the two-tailed Student's t test. Statistical significance of differences between pairs of groups in animal studies was assessed using ANOVA followed by Tukey analysis. A p value less than 0.05 was considered significant.

### **ACKNOWLEDGEMENTS**

The authors wish to acknowledge the skillful technical assistance of M. André, B. Derudas, C. Brand, A. Lucas and M. Ploton. We are indebted to M.-F. Six and the Centre d'Investigations Cliniques (C.H.R.U. Lille) for human tissue samples, to M. Brun and A. Géant (Servier) and H. Duez (INSERM U545) for mouse RNA and tissue samples and to J. Brozek (Genfit S.A.) for help with statistical analysis.

### **FUNDING**

This work was supported by research grants from Institut de Recherche Servier (IdRS), Région Nord-Pas de Calais/FEDER and Fondation Coeur et Artères. A.G, A.L., B.L. and Y.B. were supported by funds from IdRS.

## REFERENCES

1. Montague,C.T., and O'Rahilly,S. 2000. The perils of portliness: causes and consequences of visceral adiposity. *Diabetes* **49**:883-888.
2. Despres,J.P., Lemieux,I., Bergeron,J., Pibarot,P., Mathieu,P., Larose,E., Rodes-Cabau,J., Bertrand,O.F., and Poirier,P. 2008. Abdominal obesity and the metabolic syndrome: contribution to global cardiometabolic risk. *Arterioscler. Thromb. Vasc. Biol.* **28**:1039-1049.
3. Laplante,M., Festuccia,W.T., Soucy,G., Gelinias,Y., Lalonde,J., Berger,J.P., and Deshaies,Y. 2006. Mechanisms of the depot specificity of peroxisome proliferator-activated receptor gamma action on adipose tissue metabolism. *Diabetes* **55**:2771-2778.
4. Lafontan,M., and Girard,J. 2008. Impact of visceral adipose tissue on liver metabolism. Part I: heterogeneity of adipose tissue and functional properties of visceral adipose tissue. *Diabetes Metab* **34**:317-327.
5. Goldberg,R.B. 2007. The new clinical trials with thiazolidinediones--DREAM, ADOPT, and CHICAGO: promises fulfilled? *Curr. Opin. Lipidol.* **18**:435-442.
6. Heikkinen,S., Auwerx,J., and Argmann,C.A. 2007. PPARgamma in human and mouse physiology. *Biochim. Biophys. Acta* **1771**:999-1013.
7. Chao,L., Marcus-Samuels,B., Mason,M.M., Moitra,J., Vinson,C., Arioglu,E., Gavrilova,O., and Reitman,M.L. 2000. Adipose tissue is required for the antidiabetic, but not for the hypolipidemic, effect of thiazolidinediones. *J. Clin. Invest* **106**:1221-1228.
8. He,W., Barak,Y., Hevener,A., Olson,P., Liao,D., Le,J., Nelson,M., Ong,E., Olefsky,J.M., and Evans,R.M. 2003. Adipose-specific peroxisome proliferator-activated receptor  $\gamma$  knockout causes insulin resistance in fat and liver but not in muscle. *PNAS* **100**:15712-15717.
9. Jones,J.R., Barrick,C., Kim,K.A., Lindner,J., Blondeau,B., Fujimoto,Y., Shiota,M., Kesterson,R.A., Kahn,B.B., and Magnuson,M.A. 2005. Deletion of PPAR $\gamma$  in adipose tissues of mice protects against high fat diet-induced obesity and insulin resistance. *PNAS* **102**:6207-6212.
10. Tontonoz,P., Hu,E., Graves,R.A., Budavari,A.I., and Spiegelman,B.M. 1994. mPPAR gamma 2: Tissue-specific regulator of an adipocyte enhancer. *Genes Dev.* **8**:1224-1234.

11. Chawla,A., Schwarz,E.J., Dimaculangan,D.D., and Lazar,M.A. 1994. Peroxisome proliferator-activated receptor (PPAR)  $\gamma$ : Adipose- predominant expression and induction early in adipocyte differentiation. *Endocrinology* **135**:798-800.
12. Lehmann,J.M., Moore,L.B., Smith-Oliver,T.A., Wilkison,W.O., Willson,T.M., and Kliewer,S.A. 1995. An antidiabetic thiazolidinedione is a high affinity ligand for peroxisome proliferator-activated receptor gamma (PPAR $\gamma$ ). *J Biol Chem.* **270**:12953-12956.
13. Gray,S.L., and Vidal-Puig,A.J. 2007. Adipose tissue expandability in the maintenance of metabolic homeostasis. *Nutr. Rev.* **65**:S7-12.
14. Choi,K.C., Ryu,O.H., Lee,K.W., Kim,H.Y., Seo,J.A., Kim,S.G., Kim,N.H., Choi,D.S., Baik,S.H., and Choi,K.M. 2005. Effect of PPAR-alpha and -gamma agonist on the expression of visfatin, adiponectin, and TNF-alpha in visceral fat of OLETF rats. *Biochem. Biophys. Res. Commun.* **336**:747-753.
15. Laplante,M., Sell,H., MacNaul,K.L., Richard,D., Berger,J.P., and Deshaies,Y. 2003. PPAR-gamma activation mediates adipose depot-specific effects on gene expression and lipoprotein lipase activity: mechanisms for modulation of postprandial lipemia and differential adipose accretion. *Diabetes* **52**:291-299.
16. Yu,J.G., Javorschi,S., Hevener,A.L., Kruszynska,Y.T., Norman,R.A., Sinha,M., and Olefsky,J.M. 2002. The effect of thiazolidinediones on plasma adiponectin levels in normal, obese, and type 2 diabetic subjects. *Diabetes* **51**:2968-2974.
17. Sanchez,J.C., Converset,V., Nolan,A., Schmid,G., Wang,S., Heller,M., Sennitt,M.V., Hochstrasser,D.F., and Cawthorne,M.A. 2003. Effect of rosiglitazone on the differential expression of obesity and insulin resistance associated proteins in lep/lep mice. *Proteomics.* **3**:1500-1520.
18. Edvardsson,U., Bergstrom,M., Alexandersson,M., Bamberg,K., Ljung,B., and Dahllof,B. 1999. Rosiglitazone (BRL49653), a PPARgamma-selective agonist, causes peroxisome proliferator-like liver effects in obese mice. *J. Lipid Res.* **40**:1177-1184.
19. Metzger,D., Imai,T., Jiang,M., Takukawa,R., Desvergne,B., Wahli,W., and Chambon,P. 2005. Functional role of RXRs and PPARgamma in mature adipocytes. *Prostaglandins Leukot. Essent. Fatty Acids* **73**:51-58.
20. Zhu,Y., Qi,C., Calandra,C., Rao,M.S., and Reddy,J.K. 1996. Cloning and identification of mouse steroid receptor coactivator-1 (mSRC-1), as a coactivator of peroxisome

proliferator-activated receptor gamma. *Gene Expr.* **6**:185-195.

21. Gelman,L., Zhou,G.C., Fajas,L., Raspe,E., Fruchart,J.C., and Auwerx,J. 1999. p300 interacts with the N- and C-terminal part of PPAR $\gamma$ 2 in a ligand-independent and - dependent manner, respectively. *J. Biol. Chem.* **274**:7681-7688.
22. Yuan,C.X., Ito,M., Fondell,J.D., Fu,Z.Y., and Roeder,R.G. 1998. The TRAP220 component of a thyroid hormone receptor- associated protein (TRAP) coactivator complex interacts directly with nuclear receptors in a ligand-dependent fashion). *Proc. Natl. Acad. Sci. U. S. A.* **95**:14584.
23. Puigserver,P., Wu,Z., Park,C.W., Graves,R., Wright,M, Spiegelman,B.M. 1998. A cold-inducible coactivator of nuclear receptors linked to adaptive thermogenesis. *Cell* **92**(6):829-39.
24. Puigserver,P., Adelmant,G., Wu,Z., Fan,M., Xu,J., O'Malley,B., Spiegelman,B.M. 1999 Activation of PPAR $\gamma$  coactivator-1 through transcription factor docking. *Science* 286(5443):1368-71.
25. Yu,C., Markan,K., Temple,K.A., Deplewski,D., Brady,M.J., and Cohen,R.N. 2005. The nuclear receptor corepressors NCoR and SMRT Decrease peroxisome proliferator-activated receptor  $\gamma$  transcriptional activity and repress 3T3-L1 adipogenesis. *J. Biol. Chem.* **280**:13600-13605.
26. Guan,H.P., Ishizuka,T., Chui,P.C., Lehrke,M., and Lazar,M.A. 2005. Corepressors selectively control the transcriptional activity of PPAR $\gamma$  in adipocytes. *Genes Dev.* **19**:453-461.
27. Nofsinger,R.R., Li,P., Hong,S.H., Jonker,J.W., Barish,G.D., Ying,H., Cheng,S.Y., Leblanc,M., Xu,W., Pei,L. et al 2008. SMRT repression of nuclear receptors controls the adipogenic set point and metabolic homeostasis. *Proc. Natl. Acad. Sci. U. S. A* **105**:20021-20026.
28. Glass,C.K., and Rosenfeld,M.G. 2000. The coregulator exchange in transcriptional functions of nuclear receptors. *Genes Dev.* **14**:121-141.
29. Marfella,R., D',A.M., Di,F.C., Siniscalchi,M., Sasso,F.C., Ferraraccio,F., Rossi,F., and Paolisso,G. 2007. The possible role of the ubiquitin proteasome system in the development of atherosclerosis in diabetes. *Cardiovasc. Diabetol.* **6**:35.

30. Paul,S. 2008. Dysfunction of the ubiquitin-proteasome system in multiple disease conditions: therapeutic approaches. *Bioessays* **30**:1172-1184.
31. Boudjelal,M., Wang,Z.Q., Voorhees,J.J., and Fisher,G.J. 2000. Ubiquitin/proteasome pathway regulates levels of retinoic acid receptor gamma and retinoid X receptor alpha in human keratinocytes. *Cancer Res.* **60**:2247-2252.
32. Pettersson,F., Hanna,N., Lagodich,M., Dupere-Richer,D., Couture,M.C., Choi,C., and Miller,W.H., Jr. 2008. Reginoids modulate SXR activity by increasing its protein turnover in a calpain-dependent manner. *J. Biol. Chem.* **283**:21945-21952.
33. Guenther,M.G., Barak,O., and Lazar,M.A. 2001. The SMRT and N-CoR corepressors are activating cofactors for histone deacetylase 3. *Mol. Cell Biol.* **21**:6091-6101.
34. Gianni,M., Tarrade,A., Nigro,E.A., Garattini,E., and Rochette-Egly,C. 2003. The AF-1 and AF-2 domains of RAR $\gamma$  2 and RXR $\alpha$  Cooperate for triggering the transactivation and the degradation of RAR $\gamma$  2/RXR $\alpha$  heterodimers. *J. Biol. Chem.* **278**:34458-34466.
35. Prufer,K., and Barsony,J. 2002. Retinoid X receptor dominates the nuclear import and export of the unliganded vitamin d receptor. *Mol Endocrinol* **16**:1738-1751.
36. Hershko,A., and Rose,I.A. 1987. Ubiquitin-aldehyde: a general inhibitor of ubiquitin-recycling processes. *Proc. Natl. Acad. Sci. U. S. A* **84**:1829-1833.
37. Trayhurn,P., Wang,B., and Wood,I.S. 2008. Hypoxia in adipose tissue: a basis for the dysregulation of tissue function in obesity? *Br. J. Nutr.* **100**:227-235.
38. Liu,Y., Lashuel,H.A., Choi,S., Xing,X., Case,A., Ni,J., Yeh,L.A., Cuny,G.D., Stein,R.L., and Lansbury,P.T., Jr. 2003. Discovery of inhibitors that elucidate the role of UCH-L1 activity in the H1299 lung cancer cell line. *Chem. Biol.* **10**:837-846.
39. Orlicky,D.J., DeGregori,J., and Schaack,J. 2001. Construction of stable coxsackievirus and adenovirus receptor-expressing 3T3-L1 cells. *J. Lipid Res.* **42**:910-915.
40. Drenzo,J., Soderstrom,M., Kurokawa,R., Ogliastro,M.H., Ricote,M., Ingrey,S., Horlein,A., Rosenfeld,M.G., and Glass,C.K. 1997. Peroxisome proliferator-activated receptors and retinoic acid receptors differentially control the interactions of retinoid X receptor heterodimers with ligands, coactivators, and corepressors. *Mol. Cell. Biol.* **17**:2166-2176.

41. el Jack, A.K., Hamm, J.K., Pilch, P.F., and Farmer, S.R. 1999. Reconstitution of insulin-sensitive glucose transport in fibroblasts requires expression of both PPAR $\gamma$  and C/EBP $\alpha$ . *J. Biol. Chem.* **274**:7946-7951.
42. Duan, S.Z., Ivashchenko, C.Y., Whitesall, S.E., D'Alecy, L.G., Duquaine, D.C., Brosius, F.C., III, Gonzalez, F.J., Vinson, C., Pierre, M.A., Milstone, D.S. et al 2007. Hypotension, lipodystrophy, and insulin resistance in generalized PPAR $\gamma$ -deficient mice rescued from embryonic lethality. *J. Clin. Invest* **117**:812-822.
43. Setsuie, R., and Wada, K. 2007. The functions of UCH-L1 and its relation to neurodegenerative diseases. *Neurochem. Int.* **51**:105-111.
44. Takami, Y., Nakagami, H., Morishita, R., Katsuya, T., Cui, T.X., Ichikawa, T., Saito, Y., Hayashi, H., Kikuchi, Y., Nishikawa, T. et al 2007. Ubiquitin carboxyl-terminal hydrolase L1, a novel deubiquitinating enzyme in the vasculature, attenuates NF-kappaB activation. *Arterioscler. Thromb. Vasc. Biol.* **27**:2184-2190.
45. Lopez-Avalos, M.D., Duvivier-Kali, V.F., Xu, G., Bonner-Weir, S., Sharma, A., and Weir, G.C. 2006. Evidence for a role of the ubiquitin-proteasome pathway in pancreatic islets. *Diabetes* **55**:1223-1231.
46. Huss, J.M., Levy, F.H., and Kelly, D.P. 2001. Hypoxia inhibits the peroxisome proliferator-activated receptor  $\alpha$ /retinoid X receptor gene regulatory pathway in cardiac myocytes: a mechanism for O<sub>2</sub>-dependent modulation of mitochondrial fatty acid oxidation. *J. Biol. Chem.* **276**:27605-27612.
47. Lavinsky, R.M., Jepsen, K., Heinzl, T., Torchia, J., Mullen, T.M., Schiff, R., Del Rio, A.L., Ricote, M., Ngo, S., Gemsch, J. et al 1998. Diverse signaling pathways modulate nuclear receptor recruitment of N-CoR and SMRT complexes. *Proc. Natl. Acad. Sci. U. S. A.* **95**:2920-2925.
48. Zamir, I., Zhang, J., and Lazar, M.A. 1997. Stoichiometric and steric principles governing repression by nuclear hormone receptors. *Genes Dev.* **11**:835-46X.
49. Allen, T., Zhang, F., Moodie, S.A., Clemens, L.E., Smith, A., Gregoire, F., Bell, A., Muscat, G.E., and Gustafson, T.A. 2006. Halofenate is a selective peroxisome proliferator-activated receptor gamma modulator with antidiabetic activity. *Diabetes* **55**:2523-2533.
50. Reginato, M.J., Bailey, S.T., Krakow, S.L., Minami, C., Ishii, S., Tanaka, H., and Lazar, M.A. 1998. A potent antidiabetic thiazolidinedione with unique peroxisome proliferator-activated

receptor gamma-activating properties. *J. Biol. Chem.* **273**:32679-32684.

51. Germain,P., Iyer,J., Zechel,C., and Gronemeyer,H. 2002. Co-regulator recruitment and the mechanism of retinoic acid receptor synergy. *Nature* **415**:187-192.
52. Hauksdottir,H., Farboud,B., and Privalsky,M.L. 2003. Retinoic acid receptors  $\beta$  and  $\gamma$  do not repress, but instead activate target gene transcription in both the absence and presence of hormone ligand. *Mol Endocrinol* **17**:373-385.
53. Farboud,B., and Privalsky,M.L. 2004. Retinoic acid receptor-alpha is stabilized in a repressive state by its C-terminal, isotype-specific F domain. *Mol. Endocrinol.* **18**:2839-2853.
54. Carmona,M.C., Louche,K., Lefebvre,B., Pilon,A., Hennuyer,N., Audinot-Bouchez,V., Fievet,C., Torpier,G., Formstecher,P., Renard,P. et al 2007. S 26948, a new specific PPAR $\gamma$  modulator (SPPARM) with potent antidiabetic and antiatherogenic effects. *Diabetes* **55**, 2523-2533.
55. Burgermeister,E., Schnoebelen,A., Flament,A., Benz,J., Stihle,M., Gsell,B., Rufer,A., Ruf,A., Kuhn,B., Marki,H.P. et al 2006. A novel partial agonist of peroxisome proliferator-activated receptor-gamma (PPAR $\gamma$ ) recruits PPAR $\gamma$ -coactivator-1alpha, prevents triglyceride accumulation, and potentiates insulin signaling in vitro. *Mol Endocrinol* **20**:809-830.
56. Schupp,M., Clemenz,M., Gineste,R., Witt,H., Janke,J., Helleboid,S., Hennuyer,N., Ruiz,P., Unger,T., Staels,B. et al 2005. Molecular characterization of new selective peroxisome proliferator-activated receptor gamma modulators with angiotensin receptor blocking activity. *Diabetes* **54**:3442-3452.
57. Gelman,L., Feige,J.N., and Desvergne,B. 2007. Molecular basis of selective PPAR $\gamma$  modulation for the treatment of Type 2 diabetes. *Biochim. Biophys. Acta* **1771**:1094-1107.
58. Lefebvre,B., Brand,C., Flajollet,S., and Lefebvre,P. 2006. Down-regulation of the tumor suppressor gene retinoic acid receptor  $\beta$ 2 through the phosphoinositide 3-Kinase/Akt signaling pathway. *Mol Endocrinol* **20**:2109-2121.
59. Sacchetti,P., Dwornik,H., Formstecher,P., Rachez,C., and Lefebvre,P. 2002. Requirements for heterodimerization between the orphan nuclear receptor nurr1 and retinoid X receptors. *J. Biol. Chem.* **277**: 35088-35096.
60. Duez,H., Lefebvre,B., Poulain,P., Torra,I.P., Percevault,F., Luc,G., Peters,J.M.,

Gonzalez,F.J., Gineste,R., Helleboid,S. et al 2005. Regulation of human ApoA-I by gemfibrozil and fenofibrate through selective Peroxisome Proliferator-Activated Receptor $\alpha$  modulation. *Arterioscler Thromb Vasc Biol* **25**:585-591.

61. Depoix,C., Delmotte,M.H., Formstecher,P., and Lefebvre,P. 2001. Control of retinoic acid receptor heterodimerization by ligand-induced structural transitions. a novel mechanism of action for retinoid antagonists. *J. Biol. Chem.* **276**:9452-9459.

62. Forman,B.M. 2002. The antidiabetic agent LG100754 sensitizes cells to low concentrations of peroxisome proliferator-activated receptor gamma ligands. *J. Biol. Chem.* **277**:12503-12506.

63. Busch,K., Martin,B., Baniahmad,A., Martial,J.A., Renkawitz,R., and Muller,M. 2000. Silencing subdomains of v-ErbA interact cooperatively with corepressors: involvement of helices 5/6. *Mol. Endocrinol.* **14**:201-211.

64. Musti,A.M., Treier,M., and Bohmann,D. 1997. Reduced ubiquitin-dependent degradation of c-Jun after phosphorylation by MAP kinases. *Science* **275**:400-402.

65. Musti,A.M., Treier,M., Peverali,F.A., and Bohmann,D. 1996. Differential regulation of c-Jun and JunD by ubiquitin- dependent protein degradation. *Biol. Chem.* **377**:619-624.

66. Flajollet,S., Lefebvre,B., Rachez,C., and Lefebvre,P. 2006. Distinct roles of the Steroid Receptor Coactivator 1 and of MED1 in retinoid-induced transcription and cellular differentiation. *J. Biol. Chem.* **281**:20338-20348.

67. Mouchon,A., Delmotte,M.-H., Formstecher,P., and Lefebvre,P. 1999. Allosteric regulation of the discriminative responsiveness of retinoic acid receptor to natural and synthetic ligands by retinoid X receptor and DNA. *Mol. Cell. Biol.* **19**:3073-3085.

68. Bjorntorp,P., Karlsson,M., Pertoft,H., Pettersson,P., Sjostrom,L., and Smith,U. 1978. Isolation and characterization of cells from rat adipose tissue developing into adipocytes. *J. Lipid Res.* **19**:316-324.

## FIGURE LEGENDS

**Figure 1: Obese, insulin-resistant, but not lean mice respond to rosiglitazone treatment.** Male OB/OB and ob/ob mice were fed a chow diet supplemented or not (control) with rosiglitazone (RSG) corresponding to a 3mpk daily dose. A) Comparative gene expression profiles in OB/OB and ob/ob visWAT treated or not with RSG. Three samples from each group were analyzed on Affymetrix microarrays and interpreted using the Agilent Genespring GX software. These analysis are summarized here, showing the 10 most upregulated (in red) and repressed genes (in green) after the 21 days RSG treatment. The 5 most statistically significant Gene Ontology categories are indicated for each subset of genes. B) PPAR $\gamma$  is expressed in inguinal and epididymal WAT depots. Total proteins were extracted from inguinal and epididymal depots. Proteins (100 $\mu$ g) were analyzed by reducing SDS-PAGE and western blotting using anti-PPAR $\gamma$  and anti- $\beta$  actin antibodies. C) PPAR $\gamma$  target genes display enhanced responsiveness to RSG selectively in visWAT from ob/ob mice. scWAT and visWAT depots were removed from lean OB/OB, ob/ob, treated OB/OB and treated ob/ob mice. RNAs were extracted and analyzed for their content in mRNA coding for aP2, adiponectin (Adpn), glycerol kinase (GyK), PPAR $\gamma$ , Glut4 and phosphoenol pyruvate kinase (PEPCK) by RT-QPCR. Fold-inductions by RSG were calculated for each condition and are expressed as the ratio of the induction rate measured in ob/ob WAT depots to that measured in OB/OB WAT depots. (Data represent mean  $\pm$  S.E.M., \*\*p<0.01, \*\*\*p<0.005).

**Figure 2: RXR $\alpha$  protein, but not mRNA expression, is downregulated in visceral WAT from obese mice and from obese diabetic patients. .** A and B) RXR mRNA steady-state levels in mouse WAT: mRNAs from subcutaneous or visceral adipose tissues were extracted and RXR $\alpha$ , RXR $\beta$  and RXR $\gamma$  cDNAs were quantified by Q-PCR. C) RXR $\alpha$  protein in WAT sections (x10 magnification). D) RXR $\alpha$  protein in mouse WAT. Visceral (Epid.) and subcutaneous (Ing.) WAT from OB/OB mice, C57Bl6 mice fed a chow (LFD) or a high fat diet (HFD), or from ob/ob mice were probed for their content in RXR $\alpha$  and RXR $\beta$  by western blot analysis. E) and F) Quantification of data shown in D). The intensity of each RXR band was normalized to  $\beta$ actin. The first sample was arbitrarily set to 100%, and each sample was quantified relative to sample 1. (Data represent mean  $\pm$  S.E.M., \*\*\*p<0.005). G and H) RXR mRNAs steady-state levels in human WAT: mRNAs from subcutaneous and visceral adipose tissues were analyzed as in A). I) RXR $\alpha$ , RXR $\beta$  and PPAR $\gamma$  protein levels in human subcutaneous and visceral WAT. Visceral WAT from lean (LN) or obese diabetic (OD) patients was probed for their content in RXR $\alpha$ , RXR $\beta$  and PPAR $\gamma$

by western blot analysis. J), K) and L) Quantification of data shown in I). The intensity of each RXR or PPAR $\gamma$  band was normalized to  $\beta$ -actin. The first sample was arbitrarily set to 100%, and each sample was quantified relative to sample 1. (Data represent mean  $\pm$  S.E.M. \*, \*\*\* $p < 0.005$ ).

**Figure 3: Expression of UCH-L1 is upregulated in visceral WAT from obese humans and mice.**

A, B, C) Gene expression levels of UCH-L1, USP22 and WWP2 were monitored by RT-QPCR using Taqman "Assay on Demand" sets of primers. Results are expressed relative to a control sample [LN for human WAT, OB/OB (OB) for mice] arbitrarily set to 1. LN: lean normoglycemic, ON: obese normoglycemic, OI: obese glucose-intolerant, OD: obese diabetic. Ing.: inguinal, Epid.: epididymal. D) UCH-L1 protein expression in mouse WAT. Total protein extracts (50 $\mu$ g) were analyzed by western blot and immuno-probed for UCH-L1. E), F) and G) Quantification of data shown in D). The intensity of each UCH-L1 band was normalized to  $\beta$ actin. The first sample was arbitrarily set to 100%, and each sample was quantified relative to sample 1. (Data represent mean  $\pm$  S.E.M. \*,  $p < 0.05$ ; \*\* $p < 0.01$ , \*\*\* $p < 0.005$ ).

**Figure 4: RXR $\alpha$  is selectively degraded through the ubiquitin proteasome system.**

A) 3T3-L1 preadipocytes were transfected with expression vectors coding for UCH-L1, RXR $\alpha$  or RXR $\beta$ , then treated with 10 $\mu$ M MG132 or 10 $\mu$ M NH $_4$ Cl/leupeptin overnight. Whole cell extracts (WCE) were prepared 48 hours after transfection and analyzed by western blot. B) In vivo ubiquitin conjugation of RXR $\alpha$  or RXR $\beta$  in 3T3-L1 preadipocytes. Cells were transfected as above with an additional expression vector coding for HA-tagged Ub and treated as in A). WCE were submitted to immunoprecipitation with an anti-RXR antibody followed by western blot analysis of HA-conjugated proteins. C) In vitro ubiquitylation of RXR $\alpha$  and RXR $\beta$ . 50 ng of purified recombinant RXR $\alpha$  or RXR $\beta$  were incubated for 4 hours as indicated (Ub, ubiquitin 100 $\mu$ g/mL; ATP, 0.5mM; Ub-Ald, ubiquitin aldehyde 20 $\mu$ g/mL; 10 $\mu$ M MG132) and analyzed by western blotting. D) HIF transcription factor mRNAs levels in mouse visWAT. HIF1 $\alpha$ , HIF1 $\beta$ /ARNT, HIF2 $\alpha$ /EPAS and HIF2 $\beta$ /ANRT-2 mRNAs were quantified by RT Q-PCR. The level of expression in either OB/OB or LFD WAT was arbitrarily set to 1. E) Gene expression levels in 3T3-L1 adipocytes upon CoCl $_2$  treatment (4 hours). F) RXR protein levels in 3T3-L1 adipocytes upon CoCl $_2$  treatment (16 hours). G) Proteasome and UCH-L1 inhibition protect RXR $\alpha$  from CoCl $_2$ -induced degradation. 3T3-L1 adipocytes were treated for 16 hours as indicated, and WCE were analyzed by western blotting. H) Pulse-chase labeling of RXR $\alpha$  in 3T3-L1 adipocytes. Adipocytes were treated as described in the Material and Methods section. Labeled RXR $\alpha$

was immunoprecipitated and quantified by autoradiography.

**Figure 5: RXR $\alpha$  exerts a repressive effect on PPAR $\gamma$ -mediated transcription.** A) RXR and PPAR isotypes expression in differentiated 3T3-L1 adipocytes. Whole cell extracts (50 $\mu$ g) from control or RSG-treated (2 hours) cells were analyzed by western-blotting. B) Promoter occupancy by RXR and PPAR isotypes. Differentiated 3T3-L1 cells were treated as in A). RXRs, PPAR $\alpha$  or PPAR $\gamma$  association to the aP2 and the adiponectin PPRE was detected by ChIP assay. C) RXR $\alpha$  knockdown enhances PPAR $\gamma$  responsiveness to RSG in 3T3-L1 adipocytes. 3T3-L1 adipocytes were transfected with control, scrambled or anti-RXR $\alpha$  siRNAs and treated with 1 $\mu$ M RSG 24 hours later. mRNAs were assayed by Q-PCR for aP2, adiponectin (Adpn) and glycerol kinase (GyK) transcripts. Results are expressed as the ratio of mRNA level after RSG treatment to the level of mRNA expression in untreated cells. (Data represent mean  $\pm$  S.E.M. n=3, \*\*p<0.01, \*\*\*p<0.005). D) Overexpression of RXR $\alpha$  blunts the induction of PPAR $\gamma$  target genes in 3T3-L1 CAR adipocytes. 3T3-L1 CAR cells were differentiated and transduced at day 5 with either Ad-GFP, Ad-RXR $\alpha$  or Ad-RXR $\beta$ . mRNA quantification at day 7 was as in C) (Data represent mean  $\pm$  S.E.M. n=3, \*\*p<0.01, \*\*\*p<0.005). E) Expression levels of RXR isotypes in Min6, 3T3-L1, HepG2 and C2C12 cells. Total RNA from each cell type was analyzed by Q-PCR for their absolute content in RXR mRNAs. F) Min6, non differentiated 3T3-L1, C2C12 and HepG2 cells were transfected with the PPRE-driven J6 tk-Luc reporter gene and stimulated with increasing concentrations of RSG. Luciferase activities are expressed relative to the basal level of expression of the unstimulated reporter system (DMSO) arbitrarily set to 1. G) RXR $\alpha$  overexpression blunts PPAR $\gamma$  responsiveness to RSG in Min6 cells. Min6 were transfected with the J6 tk-Luc reporter gene, 30 ng of either a RXR $\alpha$  or a RXR $\beta$  expression vector, or with 15 ng of each expression vector. Luciferase activities were assayed and graphed as in F). H) RXR $\alpha$  overexpression blunts PPAR $\gamma$  responsiveness to RSG in COS cells. Experimental conditions were similar as in F). I) RXR $\beta$  confers RSG responsiveness to a positionally-restricted RXR-PPAR $\gamma$  heterodimer. PPAR $\gamma$  and mutated RXR $\alpha$  or RXR $\beta$  [both binding to a glucocorticoid response element half site; see (61)] were overexpressed in HeLa cells and the transcriptional activity of the heterodimer was monitored using a reporter gene driven by a composite GRE-PPRE or PPRE-GRE tk-Luc reporter gene. Results are expressed as in F)(Data represent mean  $\pm$  S.E.M. n=3, \*\*\*p<0.005).

**Figure 6. The ligand-dependent dismissal of SMRT from PPAR $\gamma$  depends on its association with RXR isotypes.** A) Cofactors interaction in yeast. Vectors encoding for the VP16 activating domain (AD only) or the VP16 AD in frame with the nuclear receptor interaction domain of Med1/DRIP205 (VP16-Med1), SMRT (VP16-SMRT) or NCoR (VP16-NCoR) were coexpressed with the PPAR $\gamma$  ligand binding domain fused to the Gal4 DNA binding domain. Fluorescence is expressed as arbitrary units. B) Cofactors interaction in mammalian cells. An experimental strategy similar to that described in A) was employed to monitor Med1, SMRT or NCoR interaction with the PPAR $\gamma$  LBD in HeLa cells. The basal level observed in the presence of VP16-AD and Gal4-PPAR $\gamma$  LBD was arbitrarily set to 1. C) SMRT interaction with PPAR $\gamma$  LBD in a cell-free system. A GST-SMRT fusion protein was incubated with radiolabeled PPAR $\gamma$ 1 and PPAR $\gamma$ 2, with increasing concentrations of RSG. GST-SMRT/PPAR $\gamma$  complexes were resolved by SDS-PAGE and autoradiographed. D) Corepressors interaction with  $\alpha$ P2 or adiponectin promoters in adipocytes. ChIP assays were carried out in differentiated 3T3-L1 cells to detect SMRT or NCoR loading to the  $\alpha$ P2 or adiponectin promoters. All experiments were carried out at least three times. E) Promoter occupancy by deacetylases. ChIP assays were carried out as in D) to detect either SIRT1 or HDAC3 binding to the  $\alpha$ P2 or adiponectin PPRES. Numbers indicate the relative level of binding with or without RSG (arbitrarily set to 1).

**Figure 7. RXR $\beta$  overexpression confers ligand-sensitivity to the SMRT-PPAR $\gamma$  interaction.** A) NIH 3T3 fibroblasts were transfected with expression vectors coding for the fusion protein Gal4-SMRT RID, the full length PPAR $\gamma$  fused to the VP16 activation domain (VP16-PPAR $\gamma$ ), and expression vectors coding for each RXR isotype. The full length RAR $\alpha$  fused to VP16 AD was used as a positive control. The basal level observed in the presence of the VP16-AD (AD only) and Gal4-SMRT RID was arbitrarily set to 1. The reporter gene was a pGL3-based vector containing 6 repeats of the UAS yeast sequence. B) Interaction of SMRT with the PPRE-bound PPAR $\gamma$ -RXR $\alpha$  heterodimer. NIH 3T3 cells were transfected with the expression vectors and reporter gene as in A), together with an expression vector coding either for the VP16-AD (AD only) or the VP16-AD fused to the SMRT RID (VP16-SMRT). Increasing concentrations of rosiglitazone (0, 1 or 5 $\mu$ M) were added 24 hours after transfection for 16 hours and luciferase activities were assayed and quantified as in A). The RXR $\alpha$ : RAR $\alpha$  heterodimer was used as a positive control in response to 0.5 or 1 $\mu$ M atRA. C) Interaction of SMRT with the PPRE-bound PPAR $\gamma$ -RXR $\beta$  or the PPAR $\gamma$ -RXR $\gamma$  heterodimer. Transient transfections experiments were carried out as described as in B) using either a RXR $\beta$  or a RXR $\gamma$  expression vector. (Data represent mean  $\pm$  S.E.M. n=3, \*, p<0.05, \*\*p<0.01, \*\*\*p<0.005).

## SUPPLEMENTAL DATA

**Supplementary Figure 1: Biological parameters of rosiglitazone-treated mice.** A) Blood glucose was assayed in OB/OB littermates and ob/ob mice at day 0 (D0), day 14 (D14) and day 21 (D21) treated or not (control) with RSG (3mpk). Values are indicated as a percentage of initial values measured at D0. Glycemia of OB/OB mice was ca. 140mg/dL at D0 and 200mg/dL for ob/ob mice. Blood insulin (B) and triglycerides (C) were assayed in lean OB/OB littermates and ob/ob mice at day 0 (D0), day 14 (D14) and day 21 (D21) after feeding a chow diet supplemented or not (control) with RSG (3mpk). Values are indicated as a percentage of initial values measured at D0. Mean insulin was ca. 2.0  $\mu\text{g}/\mu\text{L}$  for OB/OB mice and 4.0 $\mu\text{g}/\mu\text{L}$  for ob/ob mice. Mean TG values were ca. 70mg/dL and 90mg/dL for OB/OB and ob/ob mice respectively. Data are expressed as mean  $\pm$  S.E.M. (n=8), \*,  $p<0.05$ ; \*\* $p<0.01$ , \*\*\* $p<0.005$ ).

**Supplementary Figure 2:** In vivo ubiquitin conjugation of RXR $\alpha$  or RXR $\beta$  in 3T3-L1 preadipocytes. Cells were transfected with expression vectors coding for either RXR $\alpha$  or RXR $\beta$  and HA-tagged ubiquitin. 48 hours after transfection, cells were treated overnight with 10 $\mu\text{M}$  MG132. WCE were prepared and submitted to immunoprecipitation with an anti-HA antibody followed by western blot analysis of RXR $\alpha$  or RXR $\beta$ .

**Supplementary Figure 3: Gene expression in 3T3-L1 cells.** mRNAs levels of adiponectin, aP2 and of GyK were monitored by RT followed by real-time Q-PCR using Applied Biosystems "Assays on demand" set of primers. The expression levels are expressed relative to these in differentiated adipocytes whose values were arbitrarily set to 1. Preadipo.: Non differentiated 3T3-L1 fibroblasts; Adipo.: differentiated 3T3-L1 cells (7 days after induction); Adipo + RSG: Differentiated 3T3-L1 cells treated for 6 hours with 1 $\mu\text{M}$  rosiglitazone. (Data are expressed as mean  $\pm$  S.E.M. (n=3), \*\*\* $p<0.005$ ).

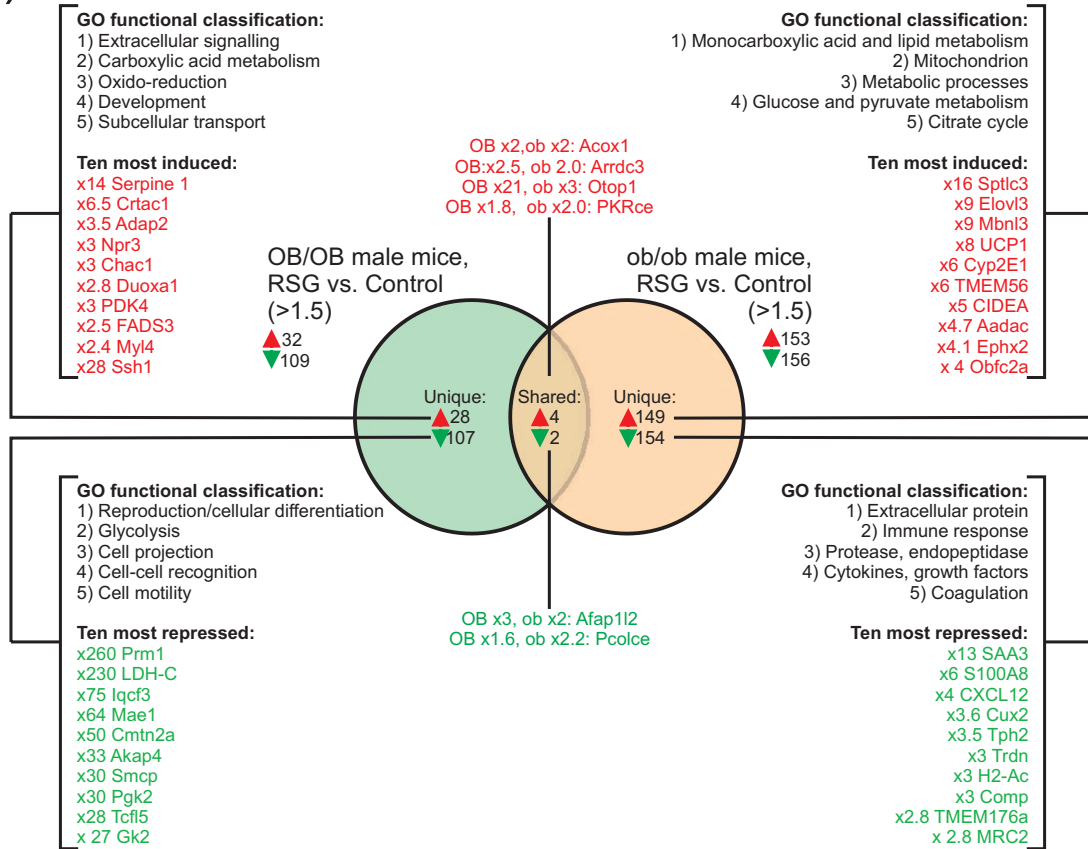
**Supplementary Figure 4: RXR $\alpha$  knockdown in 3T3-L1 adipocytes.** 3T3-L1 cells were differentiated and transfected with either a scrambled siRNA or an anti-RXR $\alpha$  siRNA as described in the Material and Methods section. The efficacy and selectivity of siRNA-mediated knockdown were assessed by RT Q-PCR quantification of RXR $\alpha$ , RXR $\beta$  and RXR $\gamma$  mRNAs (A) and by western blot analysis of whole cell extracts (B). (Data are expressed as mean  $\pm$  S.E.M. (n=3), \*\*\* $p<0.005$ ).

**Supplementary Figure 5: Adenovirus-mediated overexpression of RXR $\alpha$  or RXR $\beta$  in differentiated 3T3-L1 CAR adipocytes.** 3T3-L1 CAR were differentiated for 5 days and transduced with either an adenovirus encoding for GFP (Ad-GFP), RXR $\alpha$  (Ad-RXR $\alpha$ ) or RXR $\beta$  (Ad-RXR $\beta$ ). Two days later, cells were treated overnight with 1 $\mu$ M rosiglitazone, and 50 $\mu$ g proteins analyzed by western blotting for their content in RXR $\alpha$  or RXR $\beta$ .

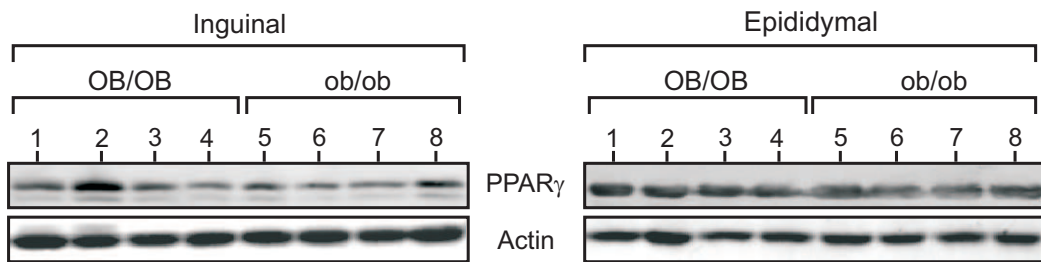
**Supplementary Figure 6: Recruitment of PPAR $\gamma$  to coactivators and SMRT.** A) SMRT interaction with monomeric PPAR $\gamma$  is insensitive to agonist challenge. Radiolabeled PPAR $\gamma$  was used as a prey in GST pulldown experiments to monitor its interaction with SMRT. B) PPAR $\gamma$  interaction with coactivators. GST pulldown experiments were carried out as in A) using PPAR $\gamma$  as a prey and GST-DRIP205, GST-GRIP1 or GST-PGC1 $\alpha$  as baits. Ligands were used at a 10 $\mu$ M final concentration.

**Supplementary Figure 7: Gene expression levels of various PPAR $\gamma$  coregulators in 3T3-L1 cells.** 3T3-L1 preadipocytes were differentiated as described in the Materials&Methods section. mRNAs from proliferating preadipocytes (P), confluent cells (C) or differentiated adipocytes (D) were extracted and analyzed by semi-quantitative RT-PCR. Amplicons were resolved on a 1% agarose gel and stained with ethidium bromide.

A)



B)



C)

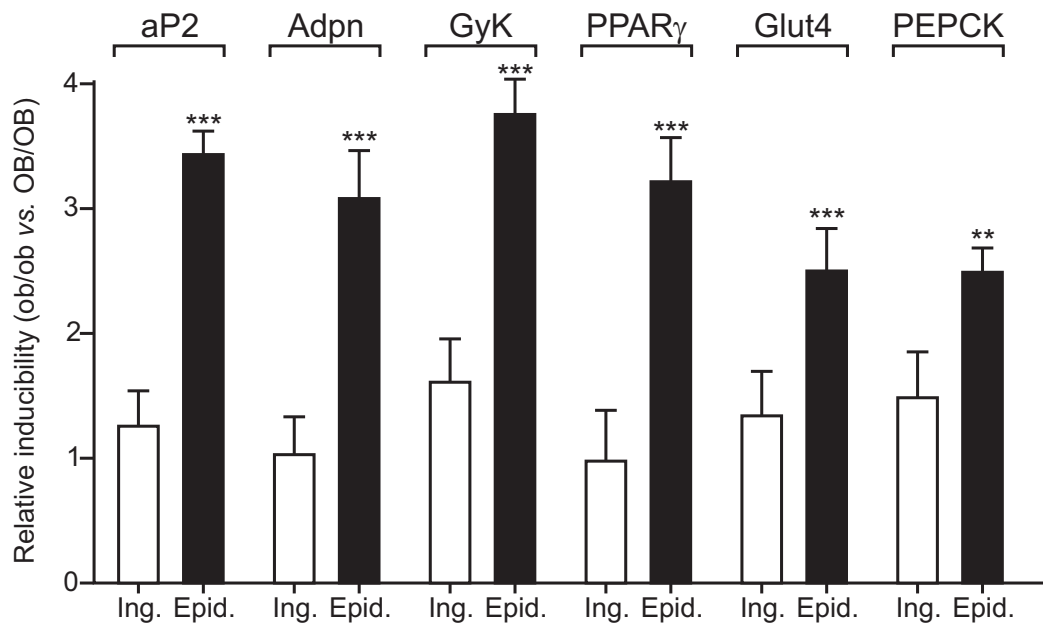
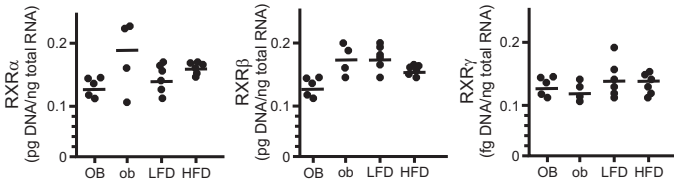
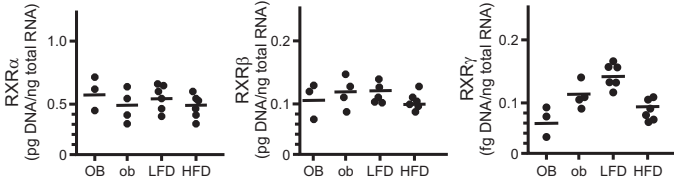


Figure 1 - Lefebvre et al.

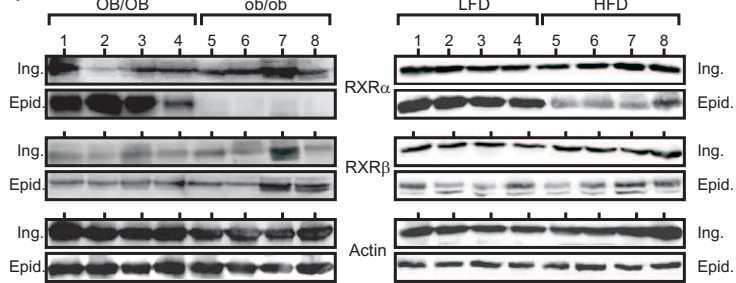
**A) Mouse inguinal WAT**



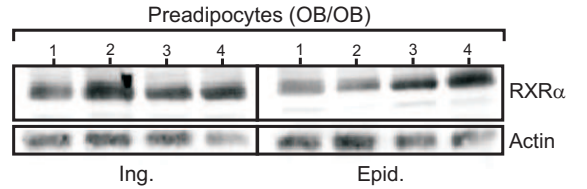
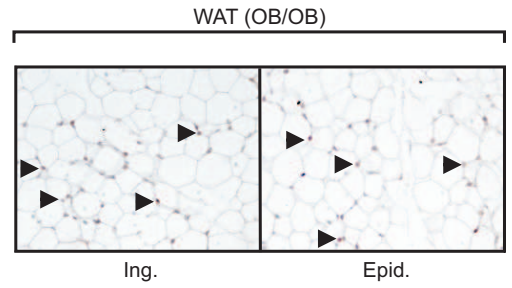
**B) Mouse epididymal WAT**



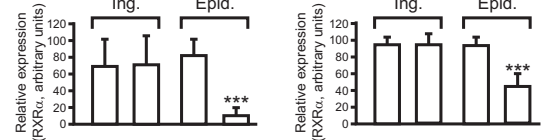
**D)**



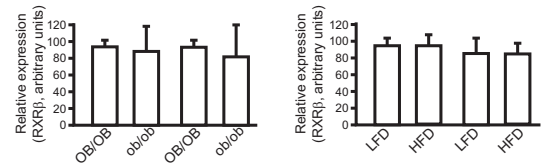
**C)**



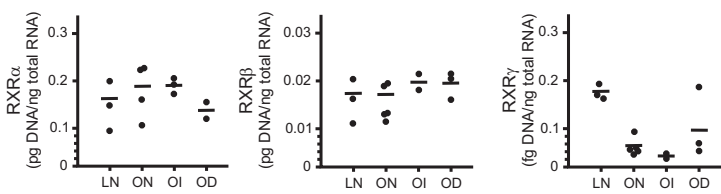
**E) RXRα**



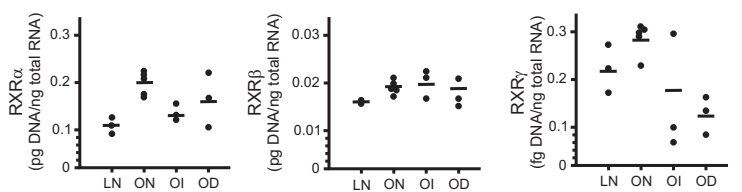
**F) RXRβ**



**G) Human subcutaneous WAT**



**H) Human visceral WAT**



**I)**

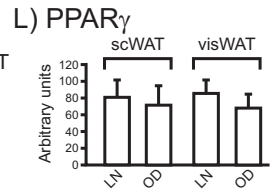
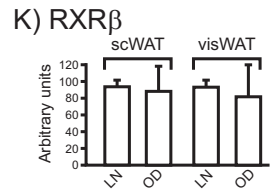
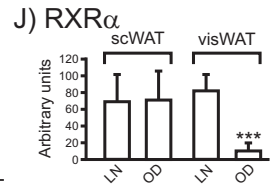
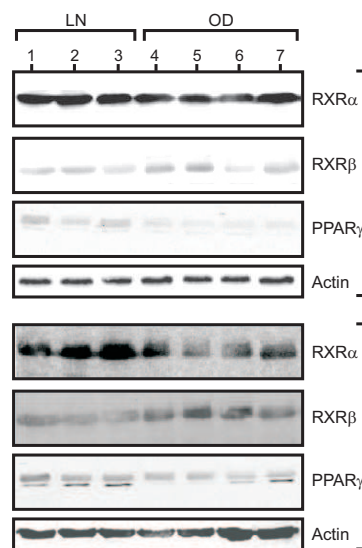
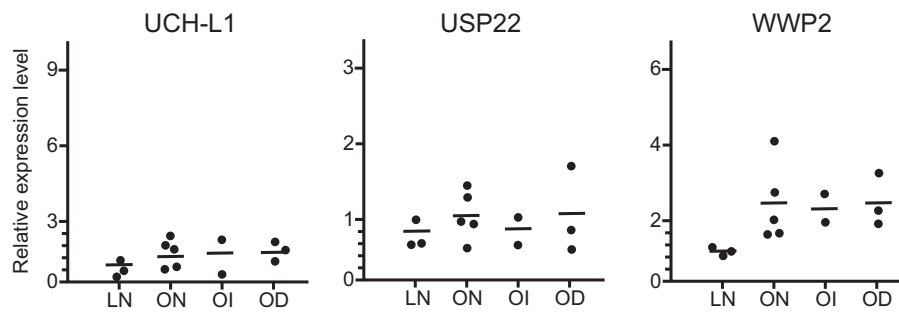
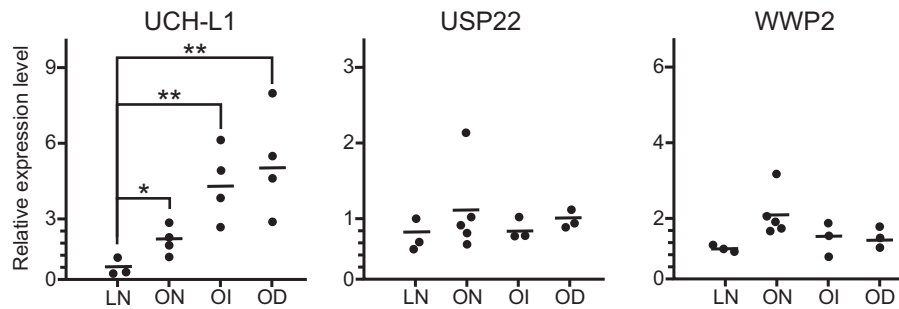


**Figure 2 - Lefebvre et al.**

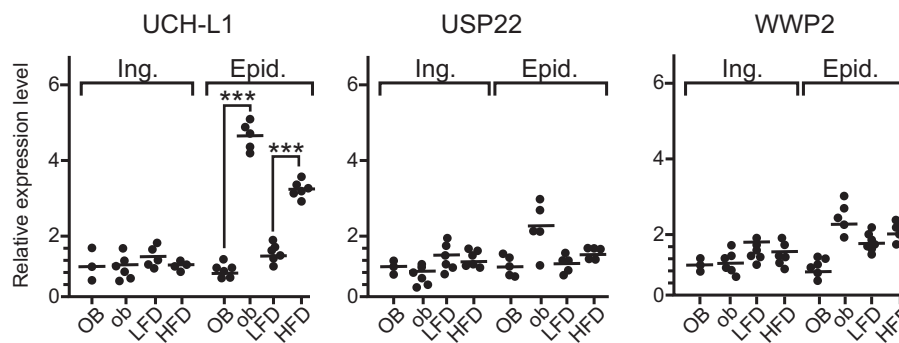
A) Human subcutaneous WAT



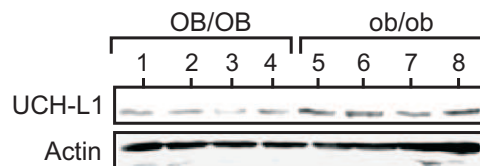
B) Human visceral WAT



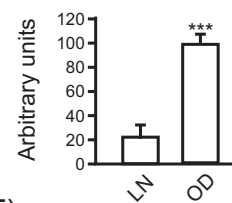
C) Mouse WAT



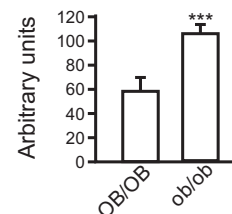
D)



E)



F)



G)

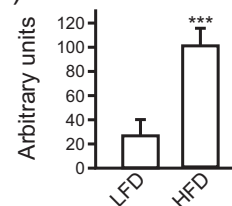
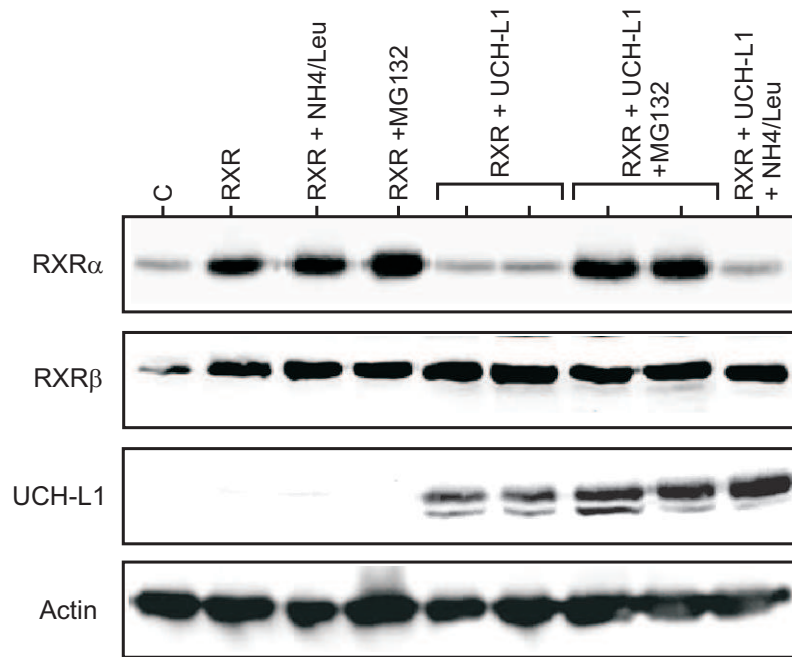
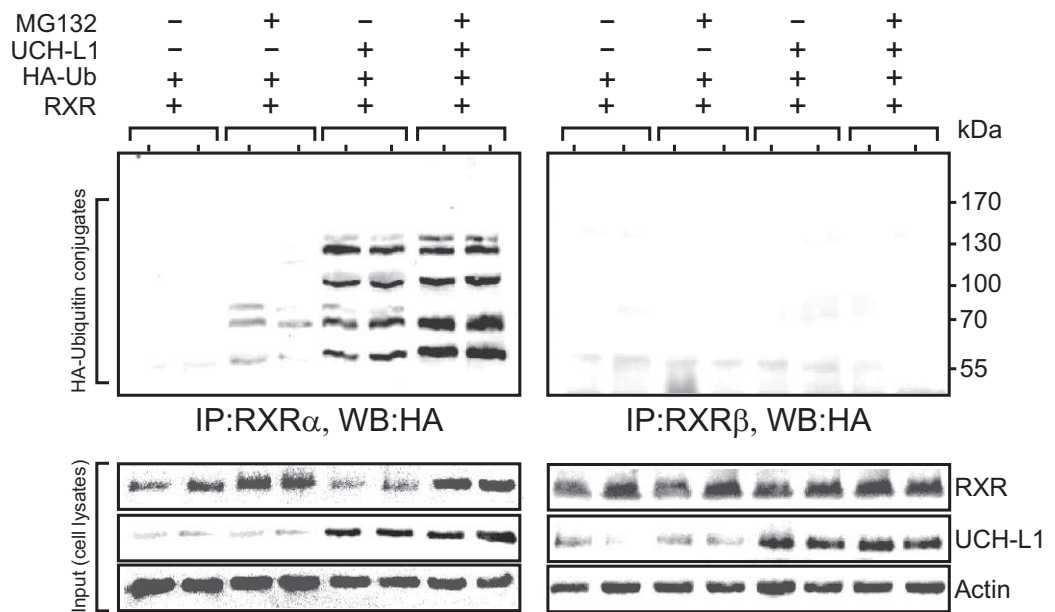


Figure 3-Lefebvre et al.

A)



B)



C)

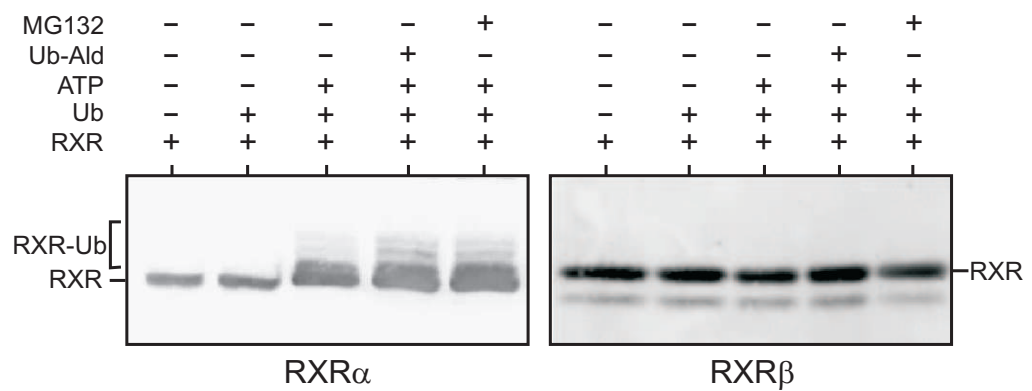


Figure 4 (A-C) - Lefebvre et al.

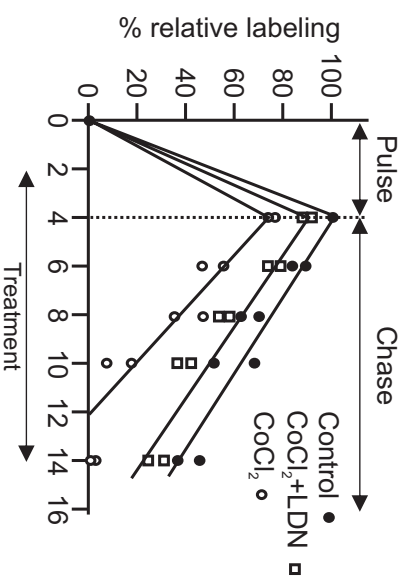
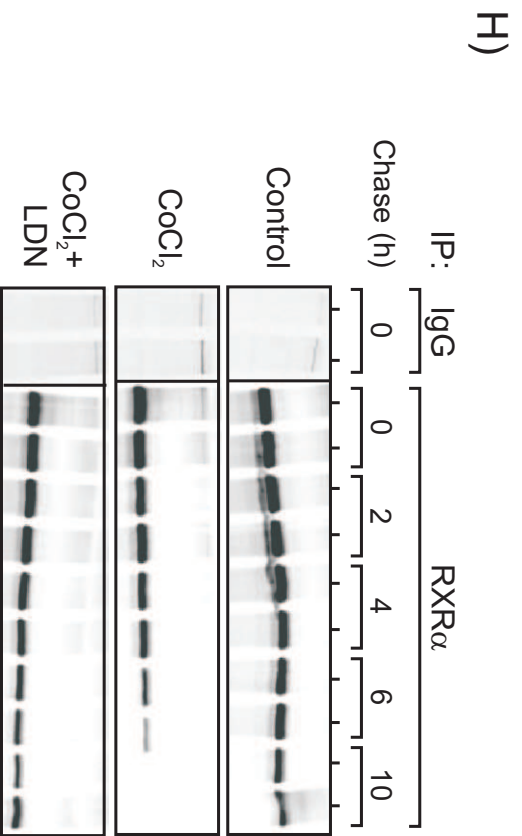
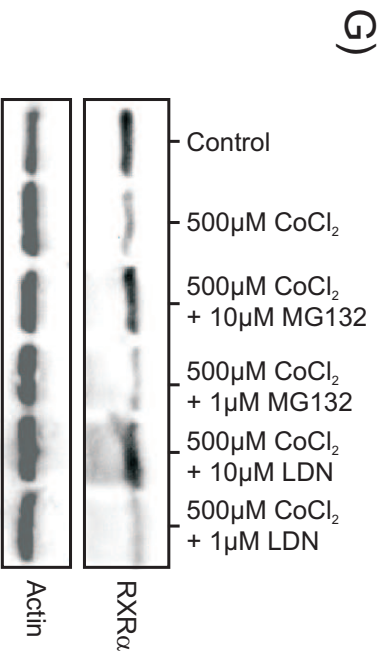
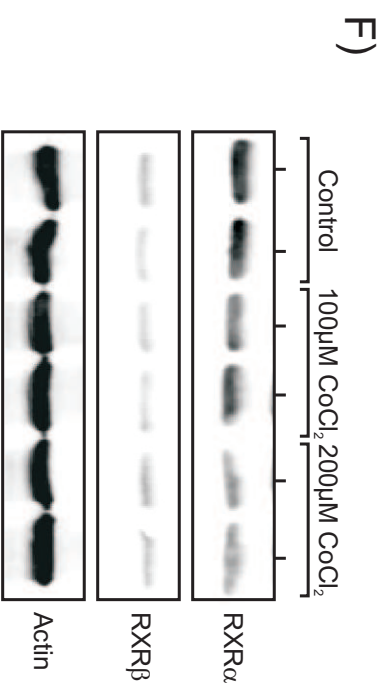
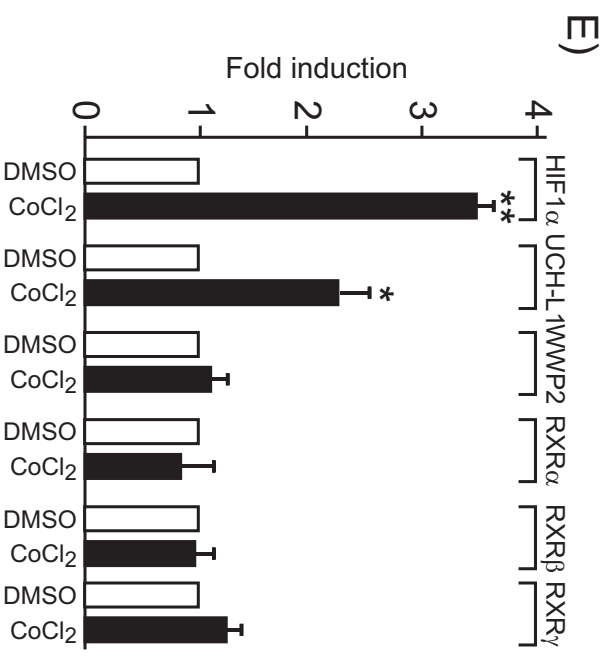
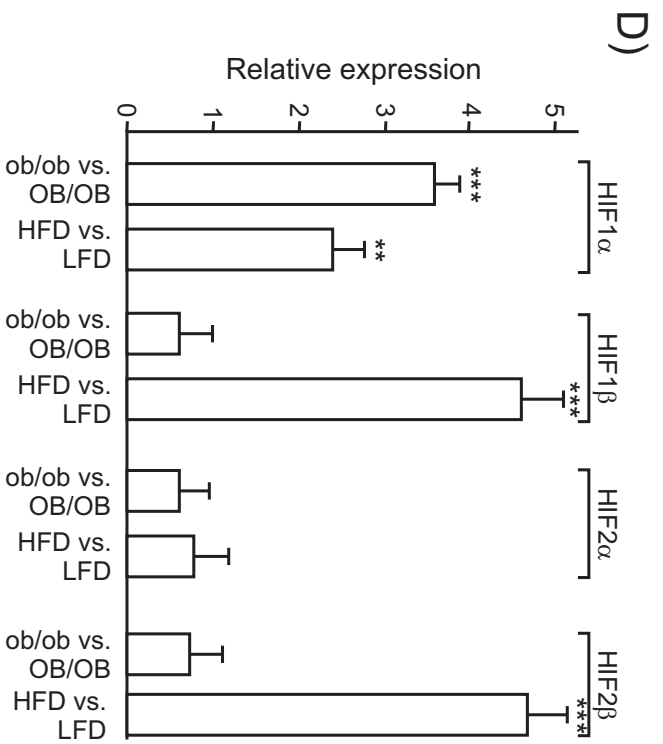
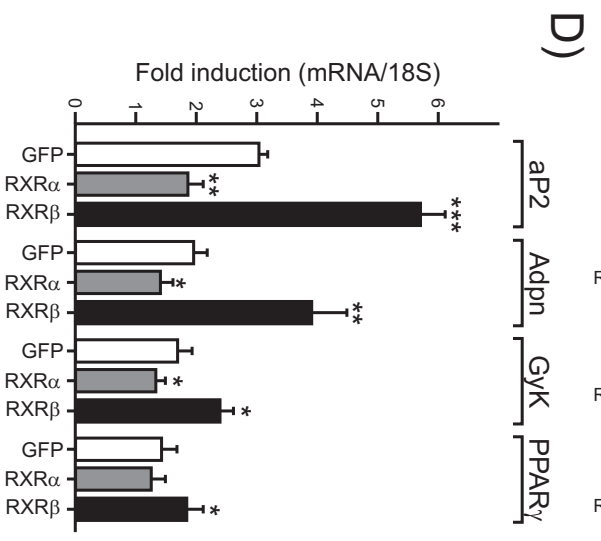
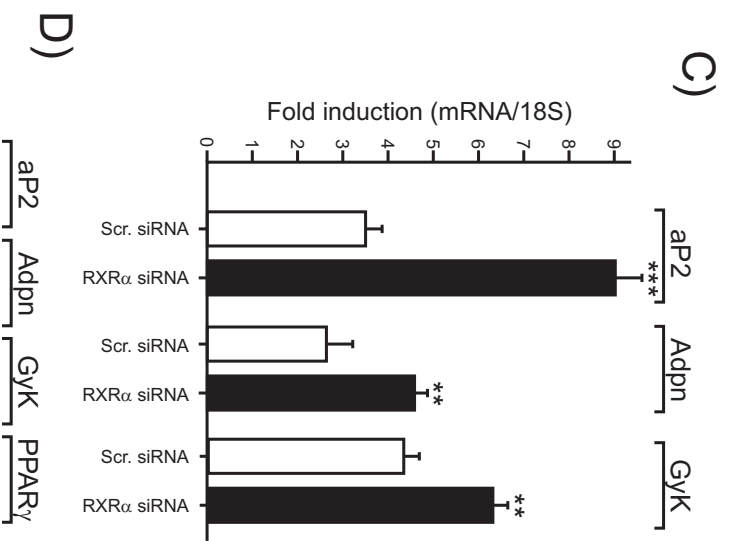
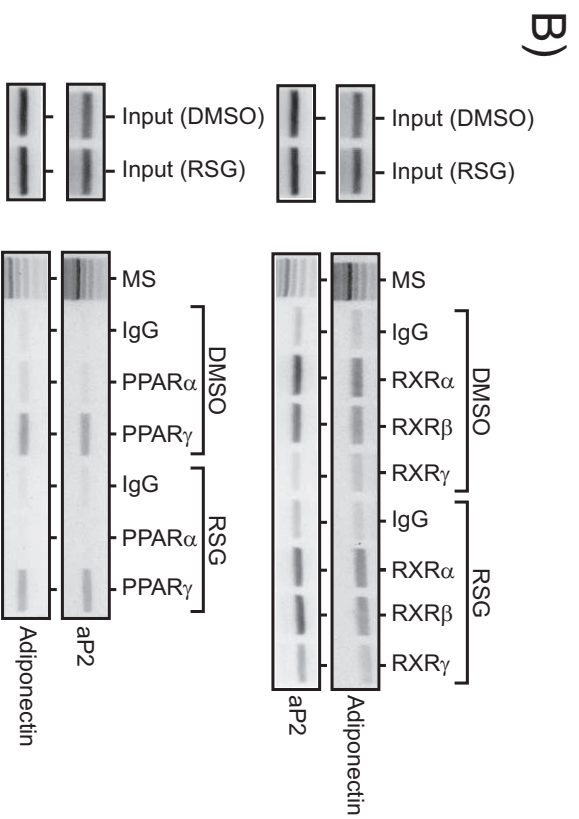
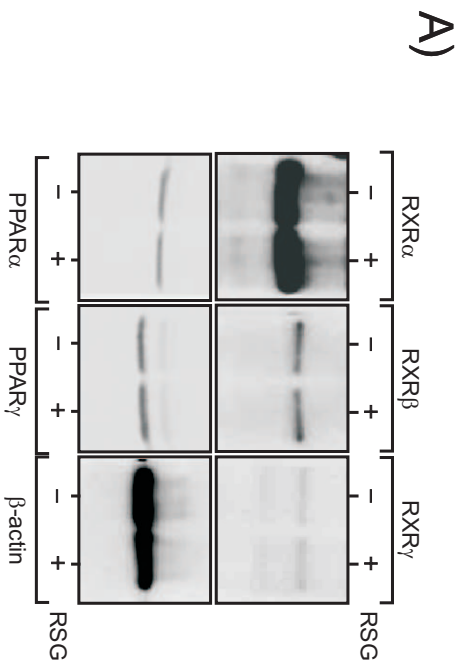
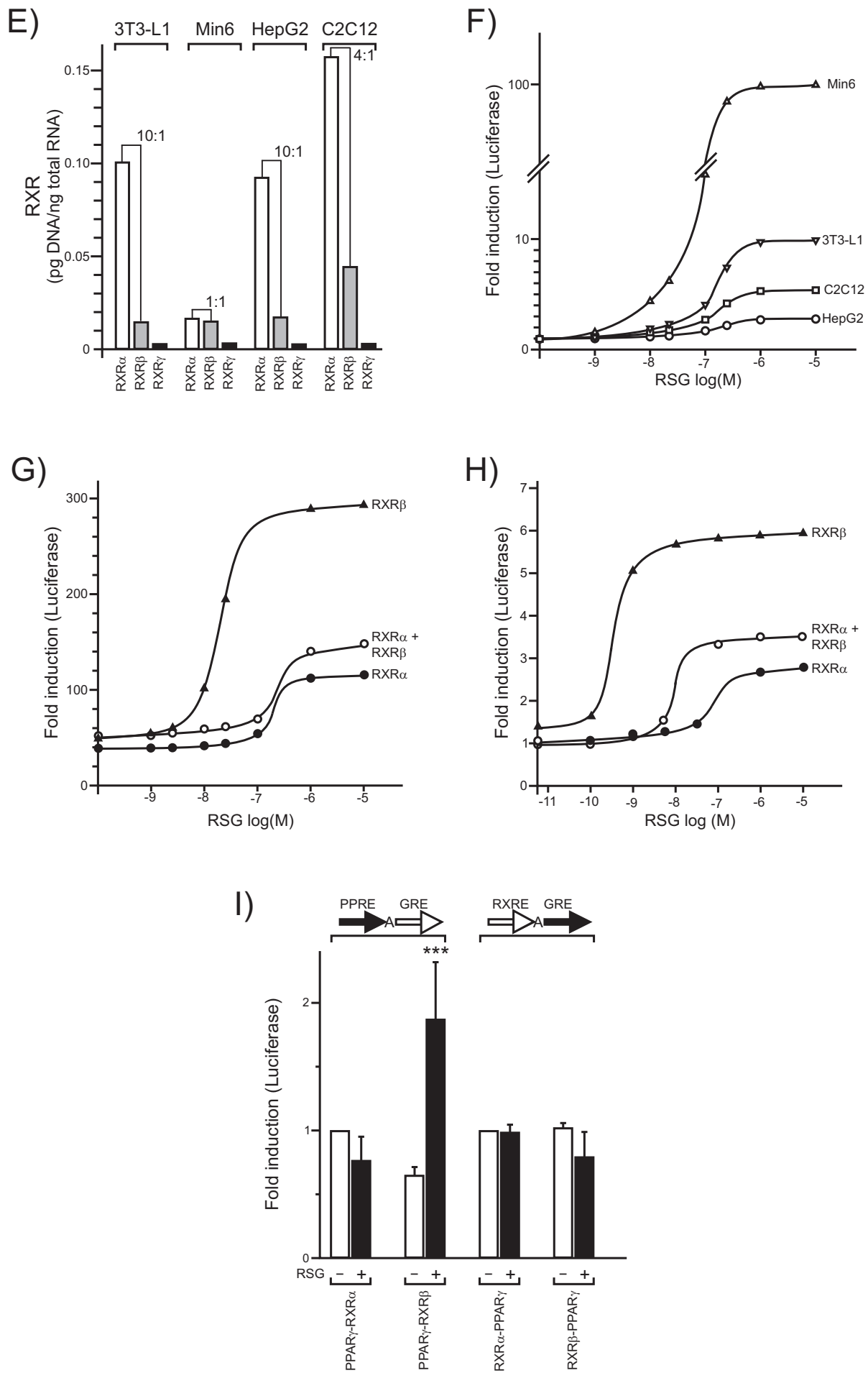


Figure 4 (D-H) - Lefebvre et al.



**Figure 5 (A-D) - Lefebvre et al.**



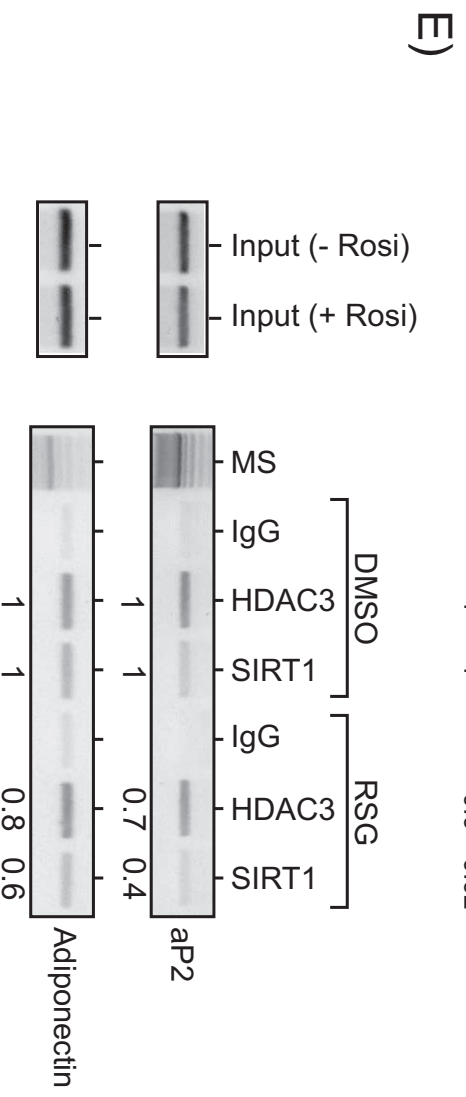
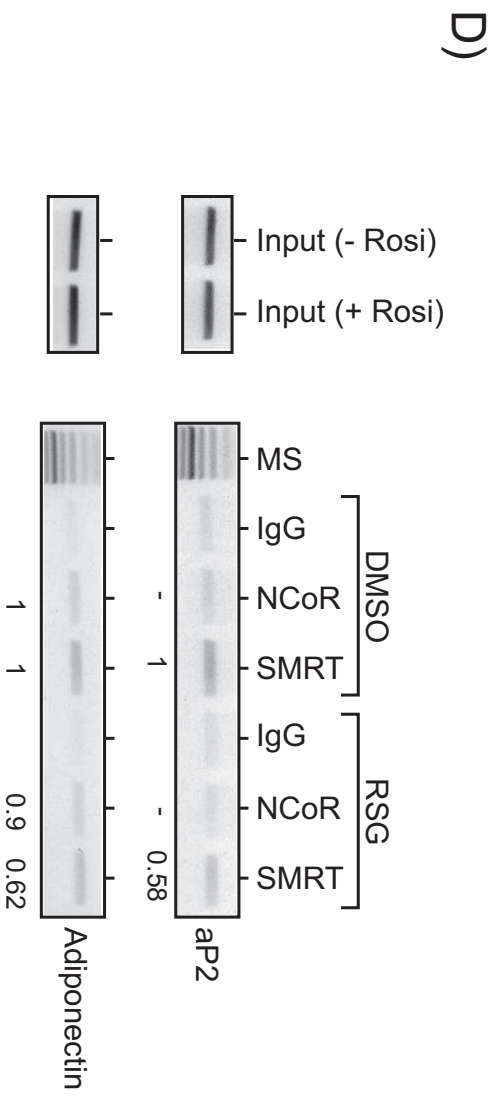
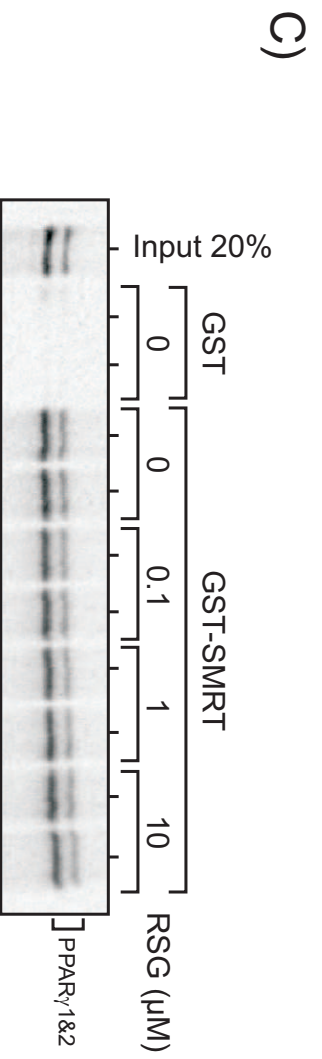
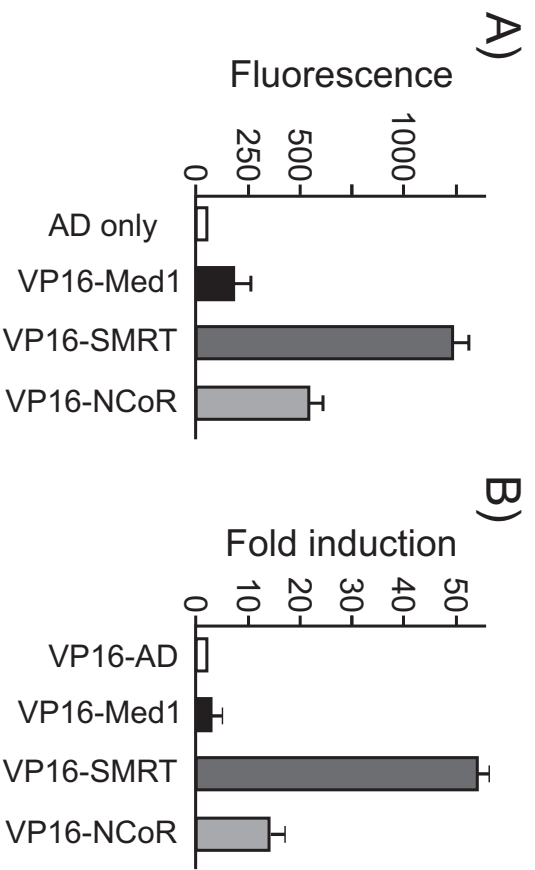
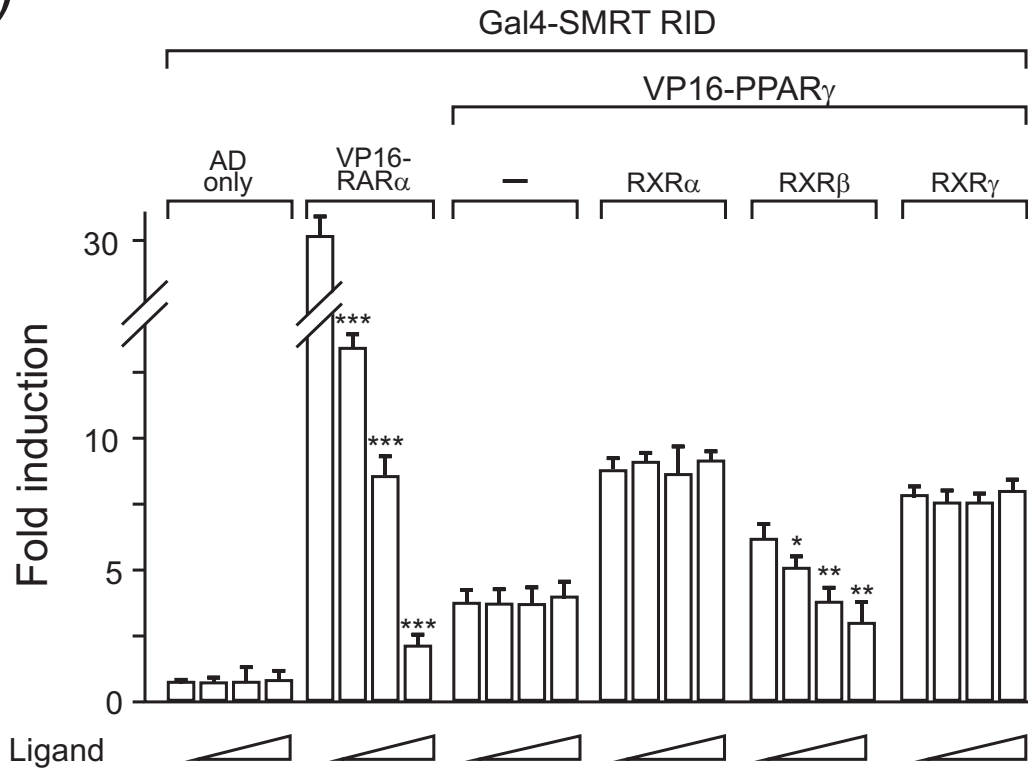
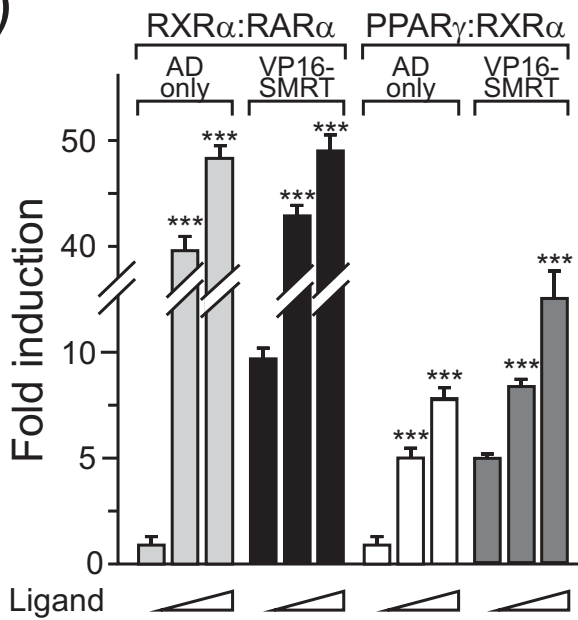


Figure 6-Lefebvre et al.

A)



B)



C)

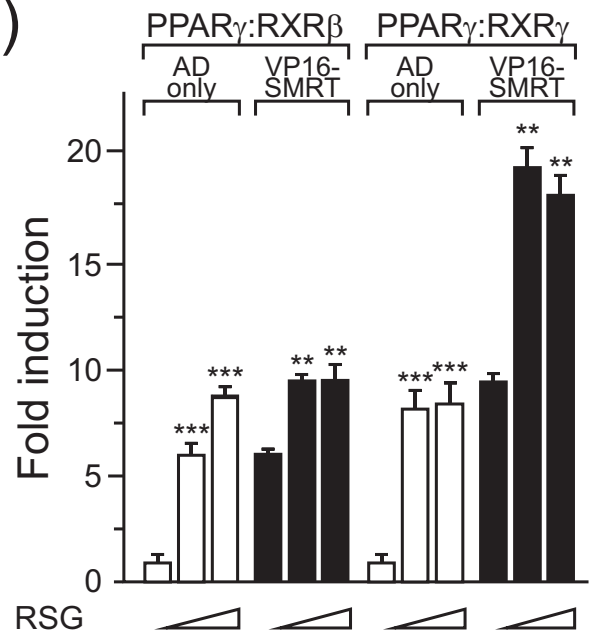
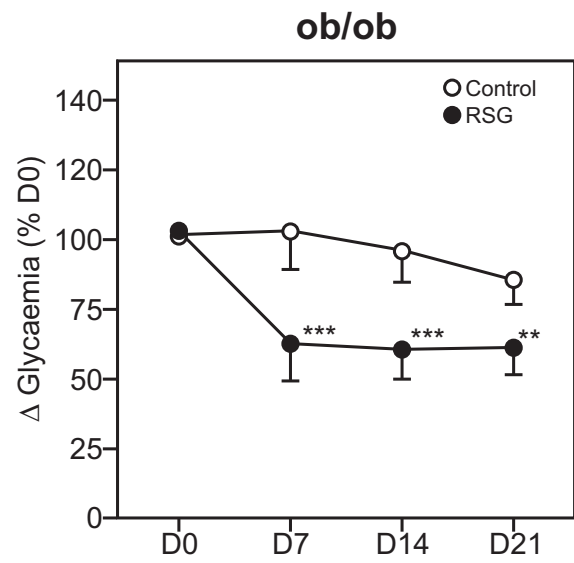
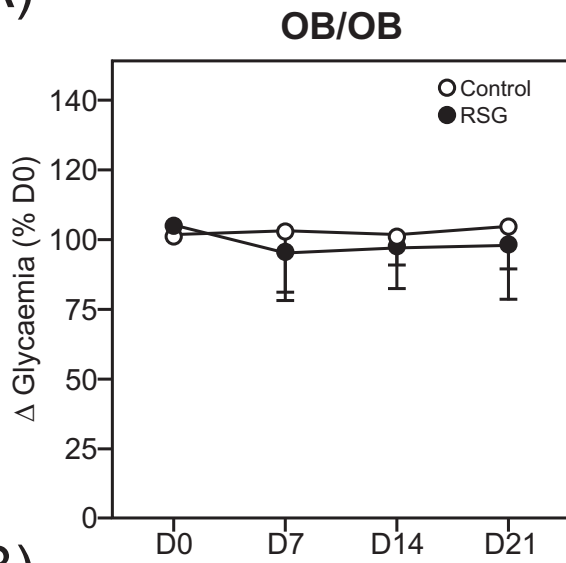
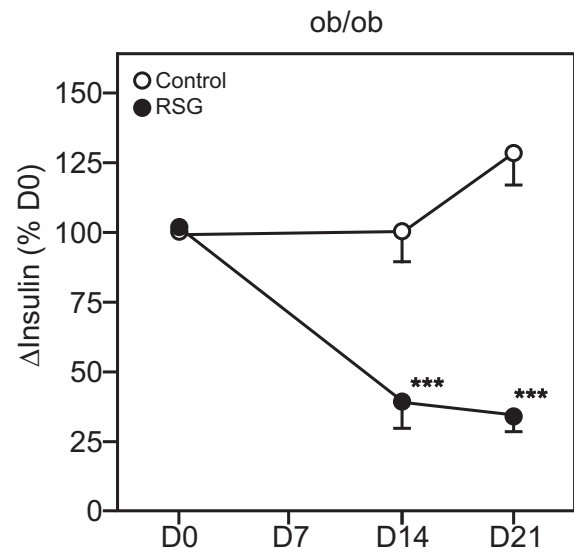
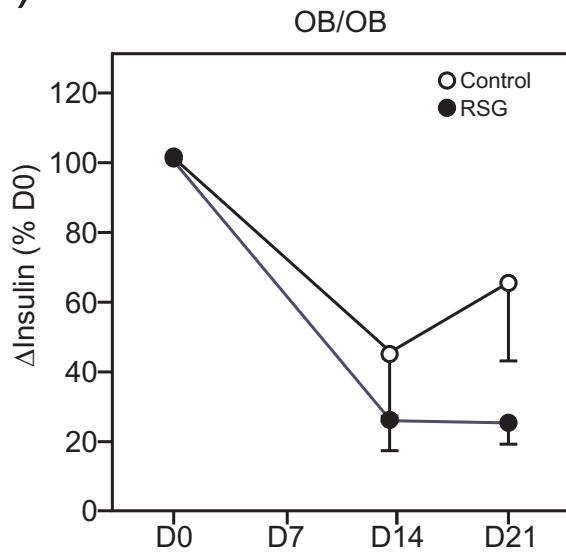


Figure 7 - Lefebvre et al.

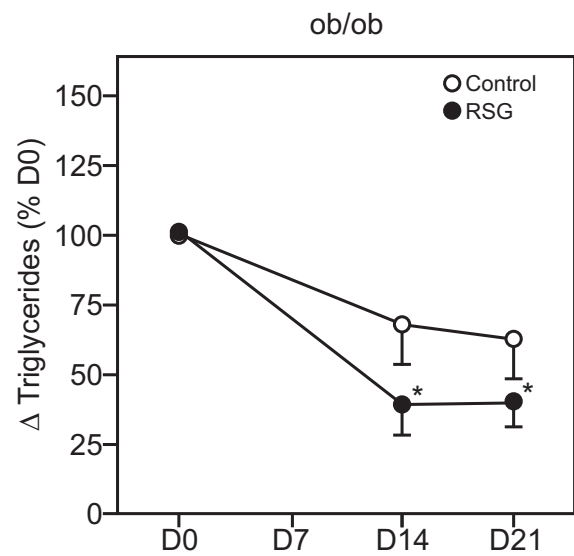
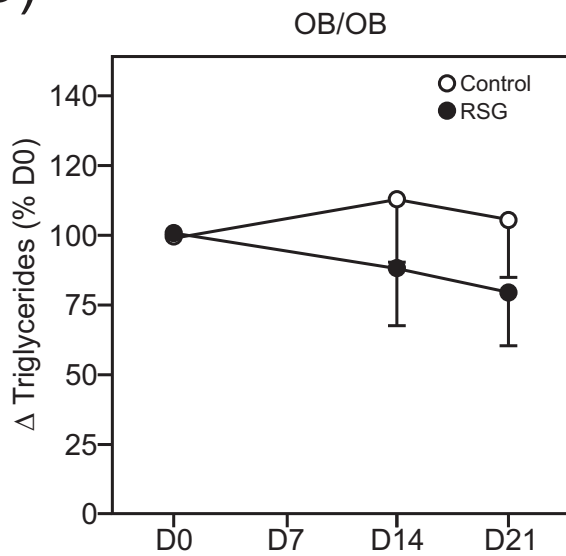
A)



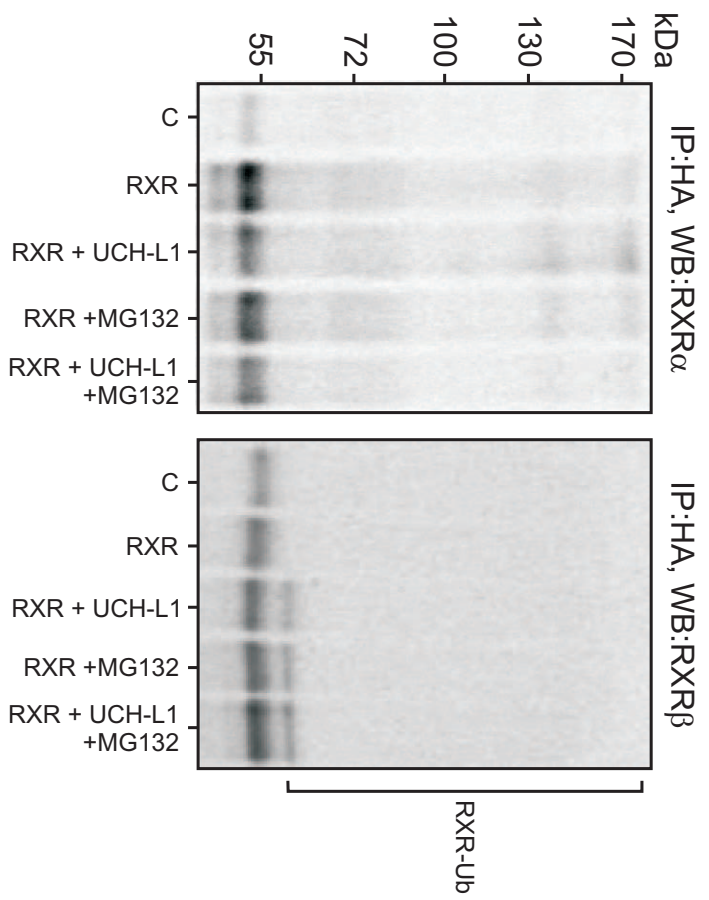
B)



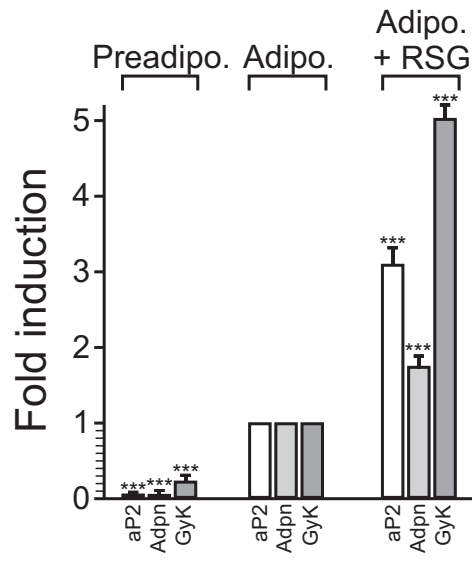
C)



Supp. Figure 1 - Lefebvre et al.

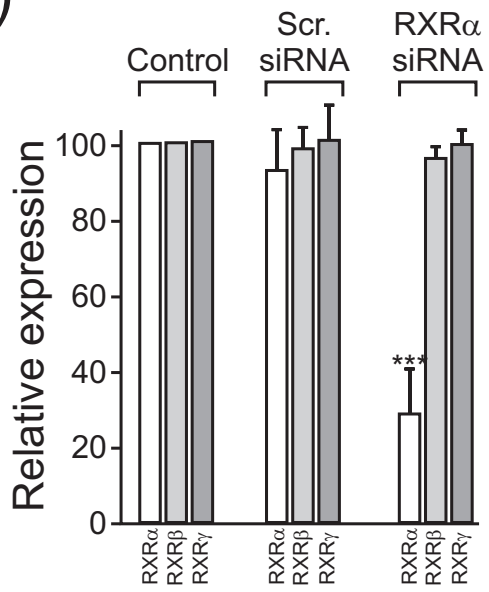


Supp. Figure 2 - Lefebvre et al.

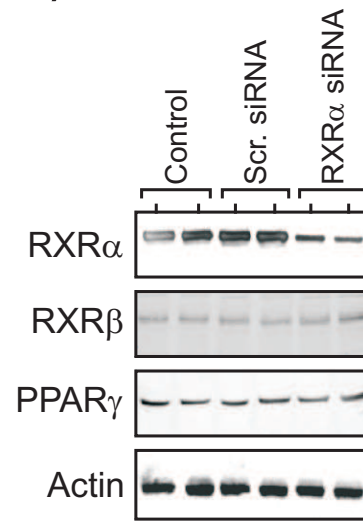


Supp. Figure 3 - Lefebvre et al.

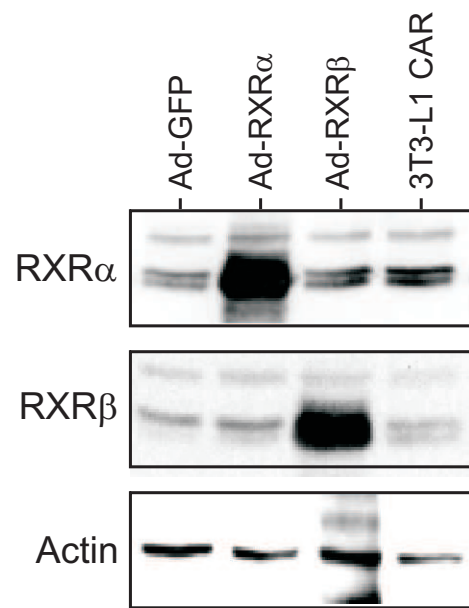
A)



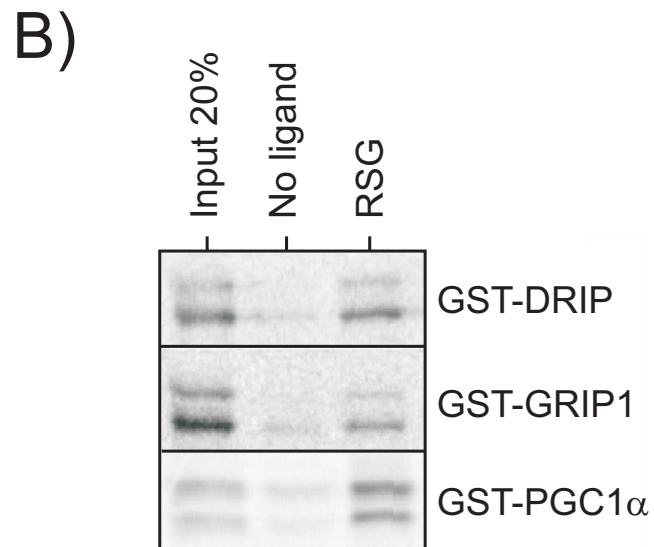
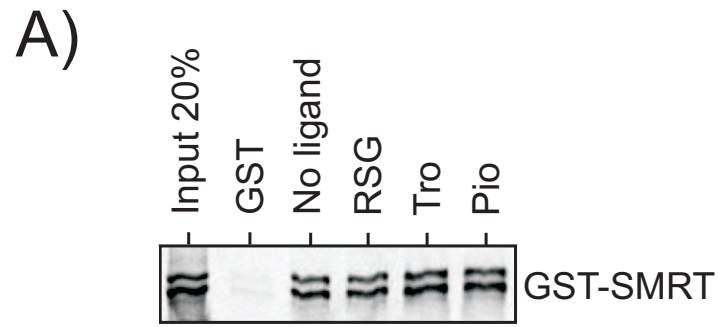
B)



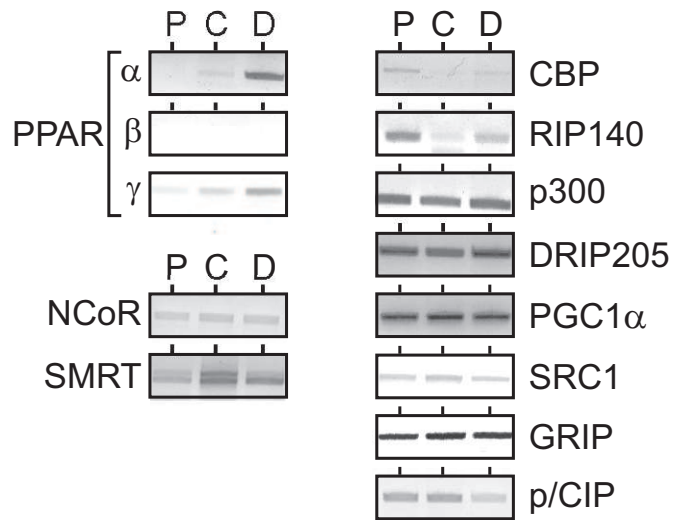
Supp. Figure 4 - Lefebvre et al.



Supp. Figure 5 - Lefebvre et al.



Supp. figure 6- Lefebvre et al.



Supp. figure 7 - Lefebvre et al.